Aircraft-Coating Weathering Studies by Analytical Methods

Arthur M. Usmani,[1] Mike Donley[2]

[1]ALTEC USA, Indianapolis, Indiana 46278
[2]Air Force Research Laboratory, Wright-Patterson Air Force Base, Ohio 45433

ABSTRACT: We predicted the life of an aircraft coating through the characterization of slightly weathered samples. To accomplish this, we completed accelerated weathering of a flat aircraft coating in a xenon-arc weather-o-meter for 0, 500, 1000, 1500, 2000, 2500, and 3000 h. Equatorial mount with mirrors for acceleration with aqua (EMMAQUA) exposures equivalent to 0, 6, 12, 18, 24, 30, 36, 42, and 48 months were also completed in this work. To determine coating-film degradation, we used electron spectroscopy for chemical analysis, also known as XPS, and $L*a*b*$ color measurement. Nonlinear regression estimations were performed on selected measurements from the test data. Two models were used. The first was the Weibull-type model. The second was a Gauss-type model that had also been used in previous work on decay processes. The second model generally provided a better fit as determined by asymptotic R^2 statistics. Secondary-ion mass spectroscopy data did not produce data consistent with decay functions. The models better described the data from color change measurements and XPS. Fourier transform infrared data fit the models but not as well as XPS and color measurement. Furthermore, data from EMMAQUA exposures fit better than data from the xenon-arc weather-o-meter. In the model development work, we used single points for both measurement and exposure. The models can be refined with a high degree of predictive precision if replicates of 10 measurements and replicates of 5 exposures are performed; we plan to report these findings in the future. © 2002 Wiley Periodicals, Inc. J Appl Polym Sci 86: 294–313, 2002

Key words: coatings; polyurethanes; ESCA/XPS; modeling

INTRODUCTION

The science of predicting the weatherability of aircraft coatings has not kept pace with the requirements of users. This work should fill the gap, however. Currently used coating test methods give limited basic information on the changes in the coating systems during weathering. These methods are inadequate for predicting long-term performance of coating systems. They can often produce erroneous and misleading results.

Current coating-requirement testing does not include coating weathering. Only initial properties, such as flexibility, solvent resistance, and color, are measured to qualify aircraft coatings. Initial properties may qualify a newly developed coating. Changes in physical properties during weathering may show some coatings are better than others. Therefore, there is a pressing need to understand property changes with weathering and aging for the aircraft coatings.

Because of environmental and workplace safety considerations as well as more demanding performance requirements by users, aircraft coatings are constantly being developed and improved. Water-based and high-solid coatings have been advanced to stages at which they have the potential of meeting the requirements. Because of newly emerged and emerging coatings, there is a need to understand the weatherability of the new coating films and their degradation mechanisms.

In weathering, coatings are subjected to elements of nature, such as solar radiation, temperature, temperature cycling, moisture, wind, and atmospheric pollutants.[1,2] The binder resins can undergo chain scission, crosslinking, hydrolysis, oxidation, and catalysis. Changes in the binder due to weathering can produce chalking and other film defects.

Therefore, there is a need to develop consistent and reliable chemical and physical characterization methods to monitor changes in performance during the exposure of aircraft coatings. More importantly, there is also a need to better understand the mechanism of coating changes during weathering; this could improve our ability to forecast the coating lifetime, help us to correctly perform repair work on weathered surfaces, and lead to better designed coating systems.[3] Understanding the initial properties of new coatings and property changes with aging will improve the qualification process and selection of coatings for the

Air Force aircraft fleet. Aerospace companies can also benefit from our work.

In this article, we describe the importance of the characterization of coatings during initial weathering, significant weathering factors, the current status of aircraft coatings, and analytical work performed on weathered samples. We also present Weibull-type and Gauss-type models that we developed in this study.

CURRENT STATUS OF AIRCRAFT COATINGS

The current U.S. market for aircraft coatings is estimated to be around $85,000,000. Topcoats for aircraft and primers are the most important segments.[4] Excellent adhesion and corrosion protection are required for aluminum, aluminum alloys, and, increasingly, advanced composites. The coatings must be resistant to phosphate ester hydraulic fluids, lubricating oils, fuels, repeated washing, and weathering. Excellent low-temperature flexibility and abrasion resistance are also required for these coatings. Coatings in current use include aliphatic polyurethane, high-solid polyurethane, aqueous polyurethane, epoxy polyamide, and self-priming coatings.

Aliphatic polyurethane coatings

Topcoats are mostly two-component polyurethane coatings. Generally, hydroxyl-terminated polyesters are used with isocyanurate trimers from hexamethylene diisocyanate or isophorone diisocyanate (IPDI). A high NCO/OH is used so that coatings moisture-cure as well. Crosslinking is accelerated with an organotin catalyst.

Polyurethanes are formed by the nucleophilic attack of the hydroxyl group against the isocyanate group to yield a substituted amide ester of carbonic acid, that is, urethane. The chemical reactions taking place in the polymerization of urethanes are complex but well understood.[5–11] The urethane linkages are considered to be the propagation reaction. When the polyol contains amine groups, a substituted urea becomes a principal product. Reactions that result in branching and crosslinking are the isocyanate–urethane that produces biuret linkages.

In exterior topcoats, aliphatic isocyanates are used that are nonyellowing, softer, and slow reacting. Because polyethers are subject to ultraviolet (UV)-catalyzed oxidative scission, they are rarely used in topcoats. Hydroxyl-functional acrylics and polyesters are the most commonly used polyols.

Therefore, in aircraft polyurethane coatings, there are many possible combinations. Catalysts, pigments, additives, and solvents can also greatly influence the linkages formed in the cure film and, therefore, performance.

Two-component polyurethane coatings result from the mixing of a polyisocyanate with a polyol just before application. On mixing, the isocyanate and polyol react immediately, resulting in a continual viscosity increase until gelation occurs.

In a recent work completed for the U.S. Air Force, *Aircraft Coating Weathering and Life Prediction Research*,[3] we determined by secondary-ion mass spectroscopy (SIMS) that the aircraft coating used in his research was a polyurethane type C with the following composition: IPDI = 2.0 mol %, diethylene glycol = 49.0 mol %, and adipic acid = 49.0 mol %.

The polyol is actually polyester made from diethylene glycol and adipic acid. IPDI is chemically 5-isocynato-1-(isocyanatomethyl)-1,3,3-trimethylcyclohexane. The introduction of isocyanurate into polyisocyanate increases the functionality and degree of crosslinking in the coating. Isocyanurates, that is, cyclic trimers, are produced from diisocyanates.

The polyol structure, functionality, and reactivity are also important. Long-chain polyols with low hydroxyl functionality give soft elastomeric polyurethanes. Short-chain polyols with higher hydroxyl functionality produce a more rigid and crosslinked high-performance coating. We determined that a polyester polyol made from diethylene glycol and adipic acid was used in the aircraft coating in our previous U.S. Air Force project. Aircraft-coating applications demand better mechanical properties. In comparison to polyether polyols, polyester polyols provide a more polar bond structure. Therefore, hydrogen-bond interactions can occur with the urethane linkages, resulting in the formation of a more cohesive polymer at room temperature with better mechanical properties.

Polyester polyols used in polyurethane coatings are low molecular weight (<3500) hydroxyl-terminated polymers produced with an excess of hydroxyl equivalents. The OH/COOH ratios may range from 2:1 to 15:14. If this ratio is close to unity, as in our case, we can expect a higher molecular weight. Furthermore, in polyester polyol synthesis, a high degree of conversion is required because the residual COOH groups from an even 99% complete conversion can retard the final cure of the polyurethane coating.

In addition to the binder, the aircraft coating contained pigments, fillers, and additives, such as catalysts and flow modifiers. On the basis of analytical results, specifically x-ray photoelectron spectroscopy (XPS), we found that rutile titanium dioxide and carbon black were used as pigments. Silica was used as the filler. Because of the presence of tin in the coating films, it appears that dibutyl tin dilaurate was used as a catalyst to enhance the room-temperature cure of the aircraft coating.

High-solid polyurethane coatings

High-solid polyurethane coatings are well established because of highly developed production and processing technology.[4] The solid contents cannot be in-

creased at will; there are certain limitations. Molecular weight, functionality, reactivity, polarity, and solubility affect application properties of the coatings. Polyisocyanates for high solids are characterized by a low molecular weight with a narrow distribution, a high NCO functionality, and a high NCO content. The same requirement holds for the polyol coreactant with respect to molecular weight and functionality.

Hexamethylene diisocyanate (HMDI) derivatives are more suited for high-solid coatings than corresponding polyisocyanates. The cyclopolymerization of both HMDI and IPDI results in isocyanurate polyisocyanates. The HMDI trimer is a liquid, whereas the IPDI trimer is a solid. The HMDI derivatives can have a pronounced influence on the coating-film properties, depending on the structure.

The stability of coating films will, of course, be influenced to a large extent by the polyol component. Any aromatic modification of either polyester or acrylic polyols would cause rapid film degradation. The polyester polyols should have a molecular weight of about 1000 with a 4–7% OH content. If these values are too low, the coatings generally deteriorate. The film hardness and resistance as well as pigment wetting and flocculation stability decrease. Acrylic polyols with 4–6% OH should have a molecular weight of about 3000; the coating deteriorates if the molecular weight is reduced much below 3000.

Aqueous polyurethane coatings

Water-based coatings have been around for many decades. The performance requirements for aircraft coatings are very demanding, and the combination of flexibility over a wide temperature range and resistance to fuel and hydraulic fluids is particularly difficult to achieve. The replacement of aliphatic polyurethanes with polyurethane dispersion-based aircraft primers and topcoats has been researched for the past 20 years. Examples are polyurethane aqueous dispersions, such as Neorez 960, crosslinked with a 0.5–2 wt % polyfunctional aziridine crosslinker, such as Cordova's XAMA 7. The dynamic mechanical analysis (DMA) of such coatings shows that the crosslink densities are low. In addition to Neorez, Hypol WB4000 also has produced suitable aircraft coatings. In aqueous dispersions, the usual pigmentation for the primer is strontium chromate, whereas titanium dioxide is used in the topcoats. The pigmentation does not affect the aqueous polyurethane dispersions.

In general, aqueous colloidal polymeric dispersions are prepared by the introduction of ionic groups into a polymer. Both anionic and cationic dispersions can be prepared. For aircraft coatings, there is also a requirement that a polymer be able to develop properties under ambient conditions. An anionic dispersion can be prepared by solubilization with a volatile base, such as ammonia or low molecular weight amines. In the process of film formation, the solubilizing agent evaporates, leaving the polymer dispersion with a free and reactive functionality.

Epoxy polyamides

Epoxy polyamides and water-reducible epoxy polyamides are useful binders for aircraft primers. Topcoats have also been prepared, but polyurethane is still the choice aircraft coating.

Self-priming coatings

Typically, coating systems for metal protection and decoration involve two or more layers. Each layer performs a desired function. The first layer, commonly called the primer, provides corrosion protection and adhesion to the metal. The next layer, known as the topcoat, provides durability, chemical resistance, gloss, and color. The chromate conversion coating is applied to aerospace alloys, such as Al 2024 T-3, before coating applications. Chromium and chromates are highly carcinogenic and cause many ailments, notably lung cancer. The U.S. Environmental Protection Agency (EPA) wants to completely eliminate toxic chromates from aircraft coatings, placing a substantial economic burden on the aerospace industry.

Self-priming coatings are directly applied to the metal in one coat that contains both chemistries.[12] Such single-layered coatings are a major improvement over multilayered coating systems. Corrosion pigments used in such coatings are nontoxic. If the coating chemistry is water-based, this type of coating will be safe for the environment and workers. We validated this concept in an EPA program and plan to report it. These coatings can protect aircraft, ships, vehicles, and support facilities. Earlier, the U.S. Navy developed organic solvent-based self-priming epoxy, alkyd, polyurethane, and acrylic coatings.[13–17]

BACKGROUND

Polymer and coating durability studies have been ongoing for about 120 years. The deterioration of coating films on outdoor exposure results from a number of factors. Elements of nature that cause property changes are light, specifically UV; water in liquid or vapor form; temperature; wind; oxygen; and atmospheric pollutants. All these factors are widely variable with the geographic location and season. The microbiological degradation of aircraft coatings is not a significant problem.

The lifetimes of polymeric coatings are now measured in years and decades. It is, however, not practical to wait for an extended period to ascertain weatherability by outdoor exposure. Furthermore, aircraft coatings should not be qualified by their initial phys-

ical properties. Data after limited natural or artificial weathering must be considered in the qualification process.

Therefore, we need methods that are rapid, accurate, and reliable for the early detection of changes and for the establishment of general relationships between the chemical and physical changes that occur early in deterioration and the ultimate performance properties.

The organic coatings not only must be resistant to changes experienced in weathering but are usually chosen with careful consideration of the demands imposed by the substrate. Large painted aluminum parts undergo considerable dimensional changes due to heating and cooling. The coating must be sufficiently elastic to withstand these dimensional changes without cracking or losing adhesion. Also, it must not swell and blister because of the condensation of moisture underneath. In aircraft coatings, the primer basically provides protection against corrosion by the transport of desirable ions and molecules to the substrate. The topcoat restricts or impedes the transport of undesirable ions, such as chloride, and provides durability and color.

Now we discuss chemical and/or physical changes that can take place during the outdoor exposure of aircraft coatings. Crosslinking increases the modulus and strength, decreases the elongation, and increases the glass-transition temperature. This can produce embrittlement, crazing, loss of adhesion under stress, and erosion. Crosslinking can be measured by DMA, swelling, stress–strain, IR, and Raman spectroscopy. Chain scissions result in a loss of strength, producing cracking, chalking, and erosion. Chain scissions can be measured by DMA and spectroscopy. Extraction leads to an increase in modulus, a reduction in elongation, a loss of low-temperature properties, and a development of voids. This produces chalking, crazing, and loss of cold flexibility. Extraction is best studied by water or solvent extraction, DMA, and stress–strain measurements. Phase changes produce changes in modulus and elongation, resulting in brittleness and loss of adhesion. DMA is an excellent method for studying phase changes. Changes in adhesion are produced by interfacial reactions leading to a loss of adhesion and binder and are best studied with scanning electron microscopy (SEM).

Methods useful for the characterization of unweathered and weathered coatings are as follows.

Chemical methods

- Reflectance and transmission IR spectroscopy.
- Laser Raman spectroscopy.
- UV spectroscopy.
- Electron spectroscopy for chemical analysis (ESCA).
- SIMS.

Physical methods

- DMA.
- Differential scanning calorimetry (DSC).
- Thermal mechanical analysis.
- Tensile (stress–strain) properties.
- Extraction and swelling.
- Water permeability.
- Gloss.
- Color ($L*a*b*$).
- Adhesion.
- Flexibility.
- Chalking.
- Surface energetics and critical contact angles.
- Conventional and environmental SEM.

Statistically, weathering is a wear-out process. Wear-out failures result from the gradual exhaustion of physical and other properties that in some way relate directly to the service lifetime of the coating. Therefore, we can accomplish the quantitative description of weathering (wear-out) data with a mathematical model.

EXPERIMENTAL

Selection of aircraft coating

Among aircraft coatings, polyurethanes are the most important. We obtained a flat polyurethane topcoat, F93A026 Gray, meeting Mil-C-85285 type I coatings from Sherwin Williams (Cleveland, OH). This coating consists of three parts urethane base, one part hardener, and one part activator. The three components were mixed, catalyzed, and reduced to 23-s Zahn #2 cup viscosity. Ten 6 in. × 12 in. panels were sprayed at a wet film thickness of 3.7–4.3 mils and cured under ambient conditions. The panels cured in about 8 h. Panels dried to a dry film thickness of 2.0–2.2 mils.

Accelerated weathering

A test that gives results in much shorter times is equatorial mount with mirrors for acceleration with aqua (EMMAQUA). Such a facility is just outside of Phoenix, AZ. This facility enhances the intensity of sunlight on the coated surface by a factor of 8 with respect to the level from direct exposure. This is achieved by the reflection of additional sunlight from rotating mirrors that follow the sun to maintain a position perpendicular to the sun's direct beam radiation at all times. For the prevention of excessive temperature buildup, a wind tunnel distributes air above and below the coated panels. A periodic spraying of water is also included in EMMAQUA.

A comparison based on equal EMMAQUA exposure energies per unit area, usually expressed as MJ m^2 (i.e., Langleys), with equal exposure in the UV

<div align="center">

TABLE I
Atom Percentage Surface Compositions of Xenon-Arc-Exposed Aircraft Coatings

</div>

Exposure time (h)	C			O	N	Sn	Ti	Si	Al	O/C	N/C
	O—C=O	C—O	CH$_2$, C—C=O								
0	10.1	12.1	49.4	23.4	2.6	—	—	2.4	—	0.327	0.036
500	11.3	8.7	41.5	29.8	6.3	—	—	2.5	—	0.485	0.102
1000	11.2	10.1	36.7	32.2	5.6	0.2	0.4	3.8	—	0.555	0.097
1500	8.0	7.8	31.9	38.5	6.1	0.7	1.0	6.1	—	0.807	0.128
2000	5.6	5.0	18.2	50.8	2.6	1.0	2.0	9.8	5.1	1.764	0.090
2500	2.4	2.5	12.7	57.9	1.3	0.9	2.4	14.2	5.6	3.290	0.074
3000	2.7	4.1	13.4	55.5	1.3	0.5	1.9	17.2	3.4	2.721	0.064

regions is reproducible, and correlation with actual exposures is possible.

There are a number of devices available for accelerated durability studies. ASTM methods G 2390 and G 5388 describe various devices. Xenon arc is superior to carbon arc, although the degradation is faster in the latter device because of the highly energetic shorter wavelength UV.

Two of the previous panels were cut to 2 in. × 5 in. for EMMAQUA. Additionally, four panels were cut to 2.5 in. × 5.5 in. for a xenon-arc weather-o-meter.

EMMAQUA is quite representative, and so we exposed our aircraft coatings to EMMAQUA for the equivalent of 0, 6, 12, 18, 24, 30, 42, and 48 months. These exposures were performed according to ASTM G90-94, Procedure B. The standard spray provides an 8-min water spray once every hour during the daylight hours when the machine is running, with an additional water spray at 9.00 p.m., 12.00 a.m., and 3.00 a.m. The previous equivalent months correspond to 0, 140, 280, 420, 560, 700, 840, 980, and 1120 MJ/m^2 UV exposure. The samples were rotated every 140 MJ/m^2 UV.

Analytics used

To determine coating-film degradation, we evaluated a number of characterization methods. These include SIMS; ESCA, also known as XPS; reflectance Fourier transform infrared (FTIR) spectroscopy; transmission FTIR; laser Raman scattering; DSC; L*a*b* color measurement; and chalking evaluation. In this work, we report the application of XPS and L*a*b* color measurement.

ESCA/XPS

ESCA measures the kinetic energy of X-ray excited photoelectrons. The escape depth of X-ray excited photoelectrons is known to be about 30 A or about 3 atomic monolayers. Because the ESCA spectrometer measures electron kinetic energy distributions, the nature of atomic species on the surface can be determined.[18–21] This technique can also measure small

binding energy shifts that can be used to determine the oxidation states of surface species. The addition of an argon-ion gun allows for depth profiling in ESCA studies.

Color measurement

During the weathering of coatings, properties such as gloss and color change, being indicative of degradation. In color calculations, tristimulus functions are used along with reflectance spectra to calculate the tristimulus values X, Y, and Z, which represent the color of a sample. The CIELAB formula is used to transform the tristimulus values into a set of three coordinates. The color coordinate values L*, a*, and b* provide a numerical representation of the color of the surface.[22,23] The color difference is obtained from the measurement of samples and a standard. A change in color, represented by ΔE, is calculated as follows:

$$\Delta E = (\Delta L^{*2} + \Delta a^{*2} + \Delta b^{*2})^{1/2}$$

Color measurements can be made with three light sources: D65, A, and F2. D65 is the most important.

RESULTS AND DISCUSSION

From XPS survey scans as well as high-resolution scans of C 1s spectra for polyurethane coatings exposed to a xenon-arc weather-o-meter for 0, 500, 1000, 1500, 2000, 2500, and 3000 h, atom percentage surface compositions were determined and are given in Table I. Results of XPS surveys and high-resolution scans of C 1s spectra for coatings EMMAQUA-exposed for up to the equivalent of 48 months are given in Table II. Results of color changes due to weathering are summarized in Table III.

Model development

Using the Statistical Analysis System or another similar program, we can determine unknown coefficients in a regression model. The properties will be dependent variables and exposure-time-independent.

TABLE II
Atom Percentage Surface Compositions of EMMAQUA-Exposed Aircraft Coatings

Equivalent months	C			O	N	Sn	Ti	Si	Al	O/C	N/C
	O—C=O	C—O	CH₂, C—C=O								
E-0	10.1	12.1	49.4	23.4	2.6	—	—	2.4	—	0.327	0.036
E-6	13.0	12.2	40.1	21.3	6.9	0.1	0.2	4.5	—	0.325	0.105
E-12	10.3	9.9	32.3	33.9	5.4	0.1	0.3	4.8	2.9	0.469	0.103
E-18	7.9	4.9	26.5	42.1	4.2	0.2	0.8	8.8	4.6	1.077	0.107
E-24	3.2	2.5	11.2	56.6	1.3	0.4	1.0	9.8	16.3	3.467	0.077
E-30	2.8	2.4	13.6	57.7	1.0	0.4	0.9	15.9	5.2	3.069	0.055
E-36	3.1	3.6	9.1	58.5	1.2	0.4	1.2	16.9	6.1	3.702	0.079
E-42	2.6	2.5	9.7	59.4	0.9	0.5	1.2	18.9	4.4	4.014	0.061
E-48	2.3	2.5	8.4	61.0	0.4	0.4	1.3	18.4	5.4	4.621	0.030

Previously used models include[24–27]

$$y = A \exp[B(t - c)]$$

$$y = K - A \exp(-Bt^2)$$

$$y = C + A \exp(-Bt^n)$$

The following relationships can be used in performing regression analyses for property data:

$$C_s = C_0 + C_1(t) + C_2(t) C_3$$

$$C_s = C_0 + C_1(t) + C_2(t)^2$$

$$C_s = C_0 + C_1(t)^{1/2} + C_2(t)^2$$

$$C_s = C_0 \exp{-C_1(t)^2} + C_2(t)$$

where C_s is the property value and t is the exposure time.

Nonlinear regression estimations were performed on selected measurements from the test data. Two models were used. The first was the Weibull-type model. The second was a Gauss-type model that had also been used in previous work on decay processes. The second model generally provided a better fit, as determined by asymptotic R^2 statistics. The models better described the data from color change measurements and XPS. FTIR data fit the models but not as well as XPS and color measurement. Furthermore, data from EMMAQUA exposure fit better than data from xenon-arc exposure.

We found that the concept of measuring coating property changes is a viable tool for predicting coating aging. We mathematically modeled the changes in aircraft-coating properties over time. The usual chemical kinetic equation is as follows:

$$Y = Y_0(1 - e^{-kt})$$

where Y is the concentration of the reaction product at time t, Y_0 is the initial concentration, and k is the rate constant.

A general mathematical form results from the Weibull distribution that has been successfully used for time-to-failure models for wear out of electron tubes and ball bearings. A Weibull-type model can be used for describing the exhaustion of certain properties of coatings caused by weathering:

TABLE III
Color Changes Due to Accelerated Weathering

Sample and exposure time	ΔL^*	Δa^*	Δb^*	ΔE
Xenon arc				
Unexposed (standard), 0 h	0.00	0.00	0.00	0.00
500	2.39	0.15	0.87	2.55
1000	5.40	0.12	1.34	5.57
1500	7.46	−0.07	1.64	7.64
2000	7.24	−0.12	1.96	7.50
2500	7.97	−0.11	2.13	8.25
3000	13.66	−0.330	2.41	13.87
EMMAQUA				
Unexposed (standard), 0 months	0.00	0.00	0.00	0.00
6	−2.01	−0.03	−0.09	2.01
12	−0.08	−0.24	0.06	0.26
18	4.50	−0.31	0.78	4.58
24	6.68	−0.40	1.18	6.68

Oxygen by Hours of Exposure

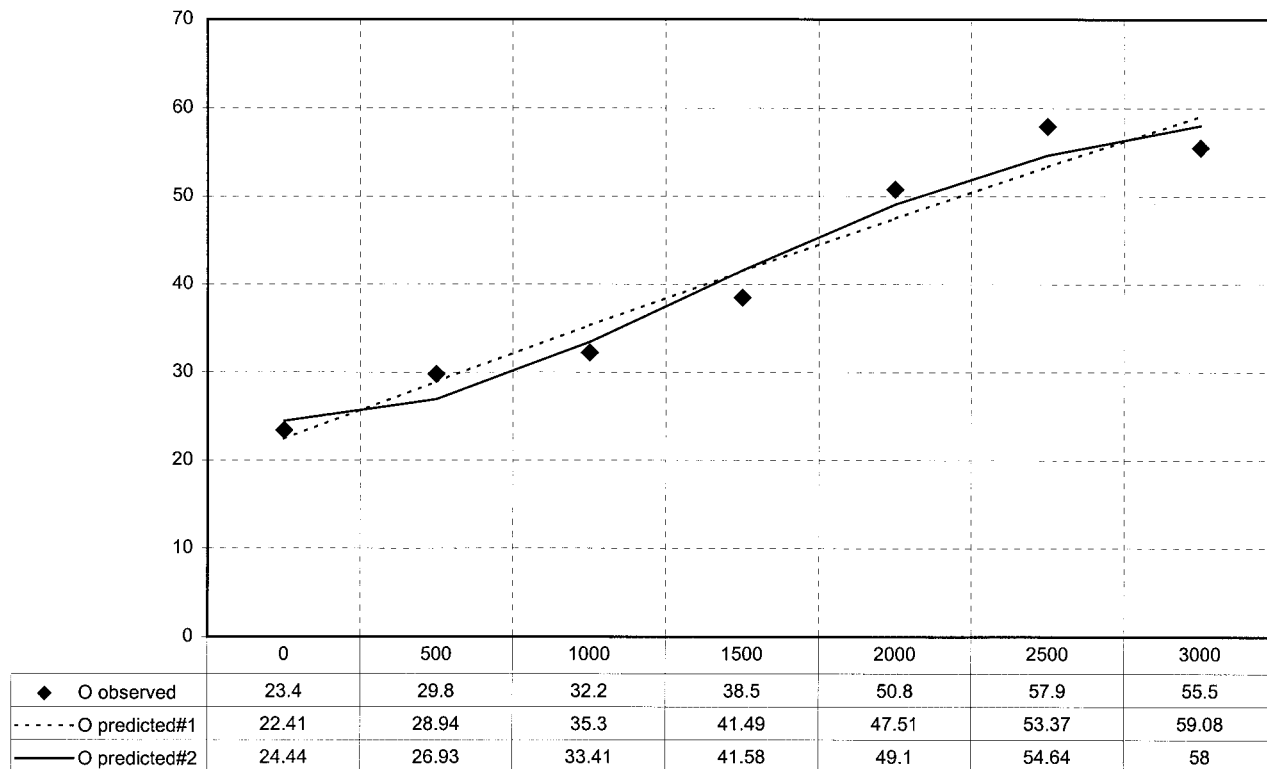|	0	500	1000	1500	2000	2500	3000
◆ O observed	23.4	29.8	32.2	38.5	50.8	57.9	55.5
- - - O predicted#1	22.41	28.94	35.3	41.49	47.51	53.37	59.08
—— O predicted#2	24.44	26.93	33.41	41.58	49.1	54.64	58

Figure 1 Oxygen by hours of xenon-arc exposure: curves and predictions of models 1 and 2.

$$Y = b_j \exp[-(t + b_2)/b_3)b_4] + b_5$$

where Y is the value of the property at time t and b_j is the parameter determined by nonlinear regression. The parameter describes the degradation curve and has physical significance. b_1 is related to the maximum property value ($b_1 = b_2 =$ maximum), b_2 is related to pre-aging and is zero in most cases, b_3 is related to the characteristic life (the exposure time that will reach 37% of the initial value), b_4 is related to the shape of the curve ($b_4 < 1$ indicates rapid initial decay and $b_4 > 1$ indicates the induction period), and b_5 is related to the asymptotic value of the property.

Nonlinear regression estimation was performed on selected measurements from the test data. Two models were used. The first was the Weibull-type model just described (with $b_2 = 0$ so that b_4 and b_4 could be independently estimated). The second model was a Gauss-type model that had also been used in previous work on decay processes:

$$Y = b_1 - b_2 \exp(-b_3 t^3)$$

The initial value is $b_1 - b_2$, the asymptotic value is b_1, and b_3 determines the curvature of the function.

The results of this analysis for xenon-arc-exposed samples are shown in Figures 1–8. These include oxygen (Fig. 1), total carbon (Fig. 2), the ratio of oxygen to carbon (Fig. 3), nitrogen (Fig. 4), the ratio of nitrogen to carbon (Fig. 5), O—C=O (Fig. 6), C—O (Fig. 7), and CH_2 + C—C=O (Fig. 8),. all by hours of exposure.

In a similar vein, the results of an analysis of EMMAQUA-exposed samples are given in Figures 9–16.

Color changes as a function of xenon-arc and EMMAQUA exposures were determined. Statistical analysis results for xenon-arc exposures are presented in Figures 17–20: Δa^* (Fig. 17), Δb^* (Fig. 18), ΔL^* (Fig. 19), and ΔE (Fig. 20). Similarly, results of EMMAQUA exposures are given in Figures 21–24: Δa^* (Fig. 21), Δb^* (Fig. 22), ΔL^* (Fig. 23), and ΔE (Fig. 24).

Data from color changes and XPS fit very well. Furthermore, EMMAQUA is superior to xenon-arc exposure because of the better fits obtained with both models. EMMAQUA-accelerated weathering closely resembles actual real-time natural weathering in comparison with xenon-arc weathering. The slight difference in EMMAQUA and xenon-arc results is due to the difference in the spectral output of light, specifically UV light. The Weibull-type model gave a good fit, but from the asymptotic R^2 statistic nonlinear regression shown in Table IV, we find that the Gauss-type model gave a slightly better fit.

Total Carbon by Hours of Exposure
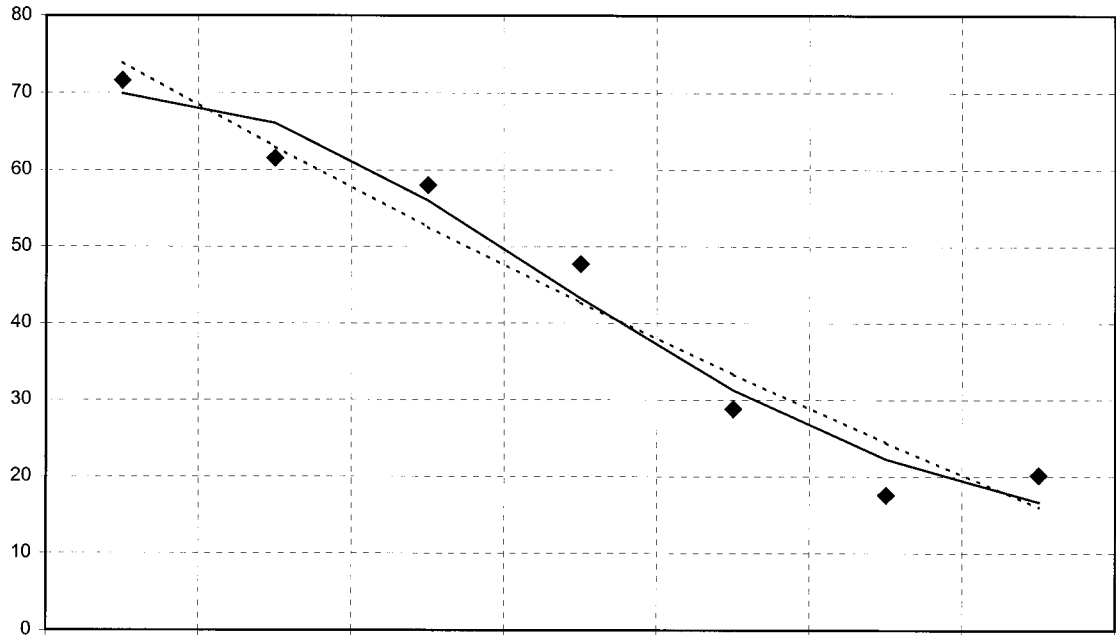
◆ C observed	71.6	61.5	58	47.7	28.8	17.6	20.2
----- C predicted#1	73.94	62.96	52.55	42.67	33.3	24.41	15.97
—— C predicted#2	69.89	66.06	56.02	43.23	31.26	22.27	16.66

Figure 2 Total carbon by hours of xenon-arc exposure: curves and predictions of models 1 and 2.

Ratio of Oxygen to Carbon by Hours of Exposure
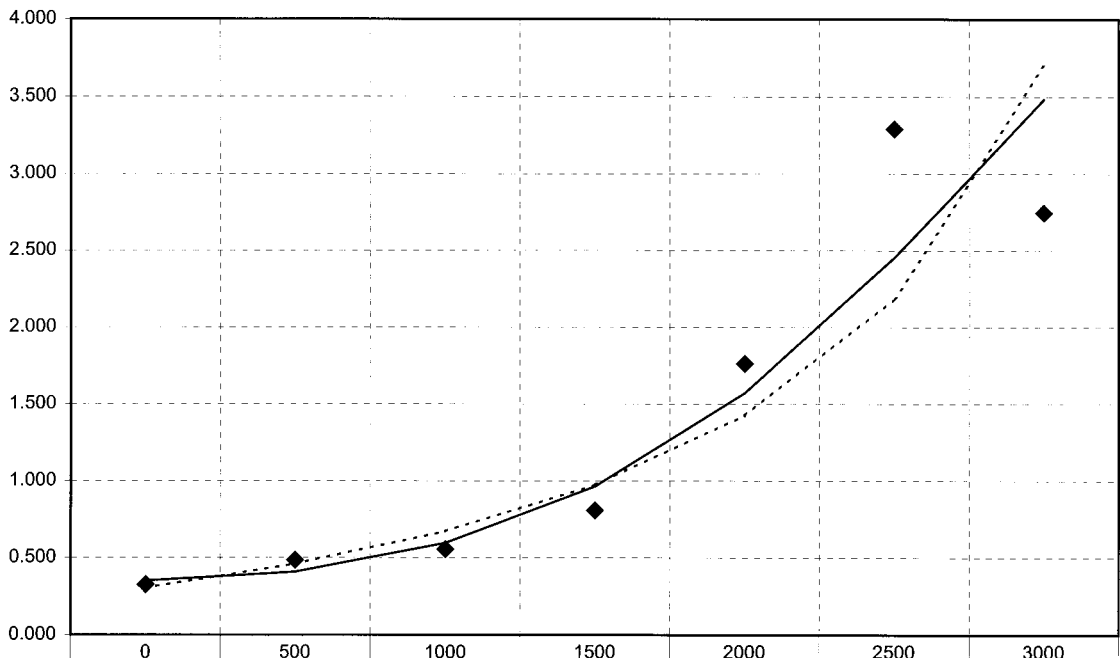
	0	500	1000	1500	2000	2500	3000
◆ O/C observed	0.327	0.485	0.555	0.807	1.764	3.290	2.748
----- O/C predicted#1	0.303	0.460	0.672	0.972	1.427	2.186	3.699
—— O/C predicted#2	0.350	0.408	0.596	0.962	1.571	2.454	3.481

Figure 3 O/C by hours of xenon-arc exposure: curves and predictions of models 1 and 2.

Nitrogen by Hours of Exposure

	0	500	1000	1500	2000	2500	3000
◆ N observed	0	6.3	5.6	6.1	2.6	1.3	1.3
- - - N predicted#1	8.13	6.86	5.62	4.42	3.25	2.12	1.01
—— N predicted#2	6.94	6.65	5.83	4.63	3.28	1.97	0.84
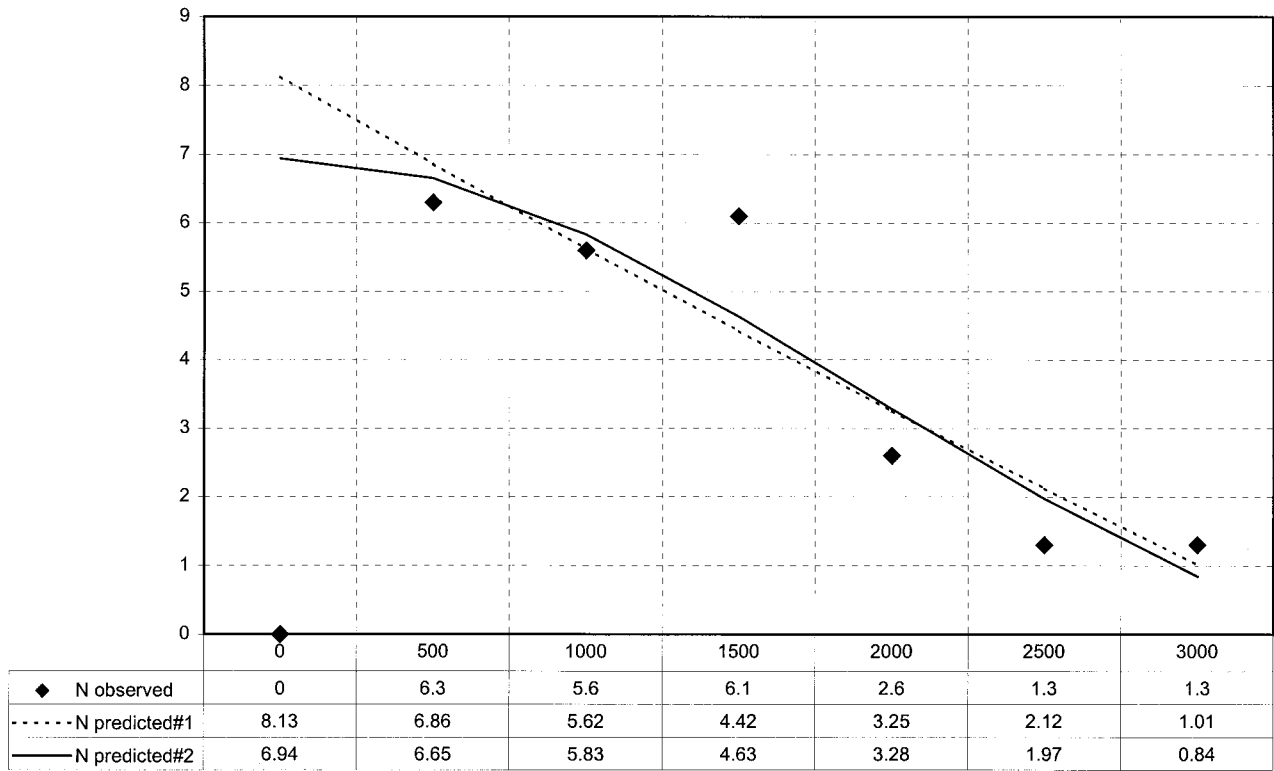
Figure 4   Nitrogen by hours of xenon-arc exposure: curves and predictions of models 1 and 2.

Ratio of Nitrogen to Carbon by Hours of Exposure

	0	500	1000	1500	2000	2500	3000
◆ N/C observed		0.102	0.097	0.128	0.090	0.074	0.064
- - - N/C predicted#1	0.110	0.109	0.107	0.104	0.098	0.087	0.063
—— N/C predicted#2	0.099	0.101	0.104	0.107	0.105	0.088	0.050
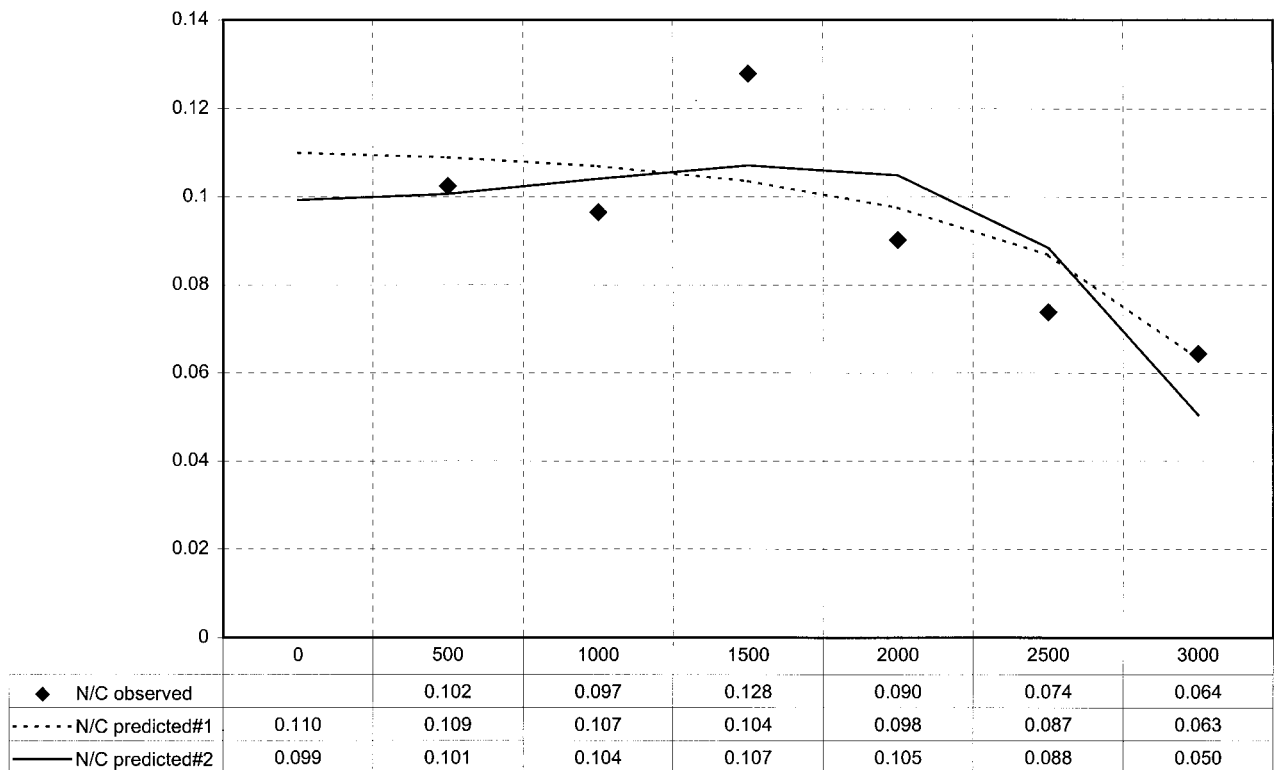
Figure 5   N/C by hours of xenon-arc exposure: curves and predictions of models 1 and 2.

O-C=O by Hours of Exposure

	0	500	1000	1500	2000	2500	3000
◆ OCO observed	10.1	11.3	11.2	8	5.6	2.4	2.7
----OCO predicted#1	12.25	10.59	8.94	7.32	5.71	4.13	2.57
—OCO predicted#2	11.45	10.99	9.7	7.83	5.72	3.68	1.94
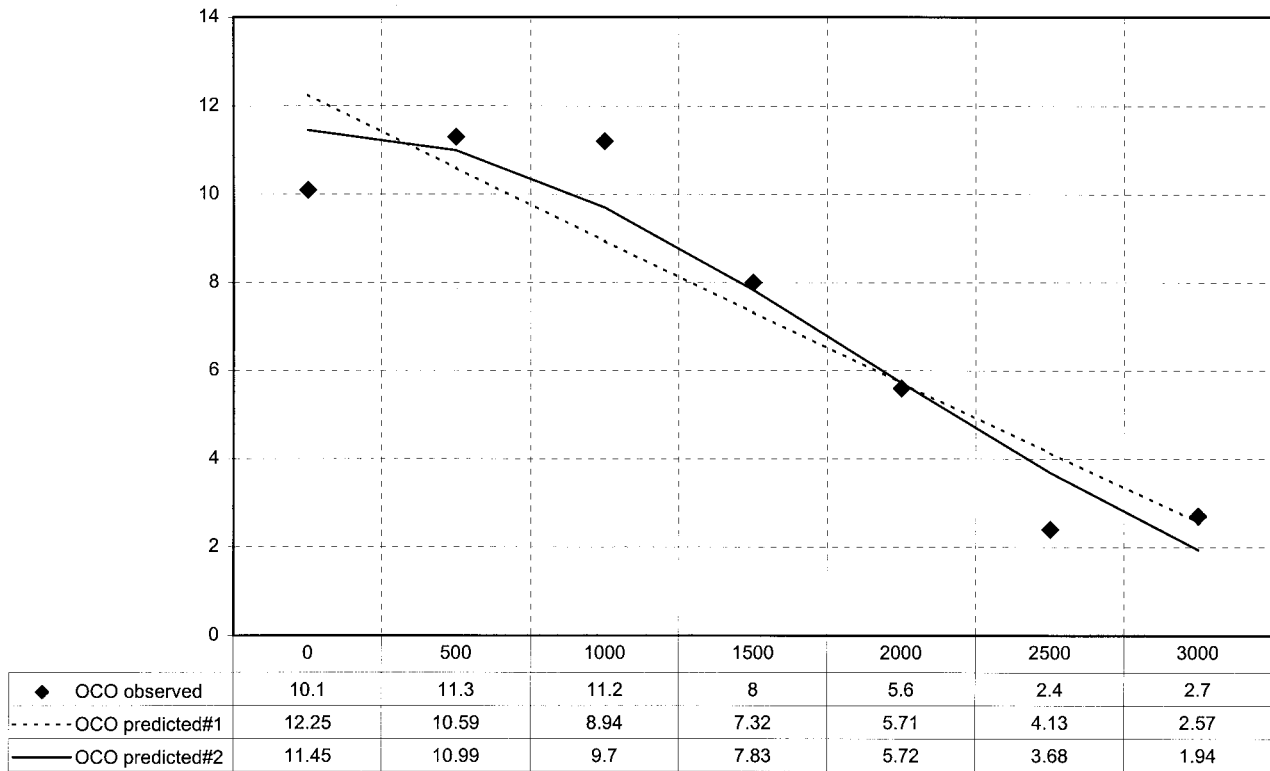
Figure 6 O—C=O by hours of xenon-arc exposure: curves and predictions of models 1 and 2.

C-O by Hours of Exposure

	0	500	1000	1500	2000	2500	3000
◆ CO observed	12.1	8.7	10.1	7.8	5	2.5	4.1
----CO predicted#1	11.86	10.15	8.53	7.01	5.57	4.23	2.96
—CO predicted#2	11.22	10.62	9.06	7.09	5.27	3.93	3.11
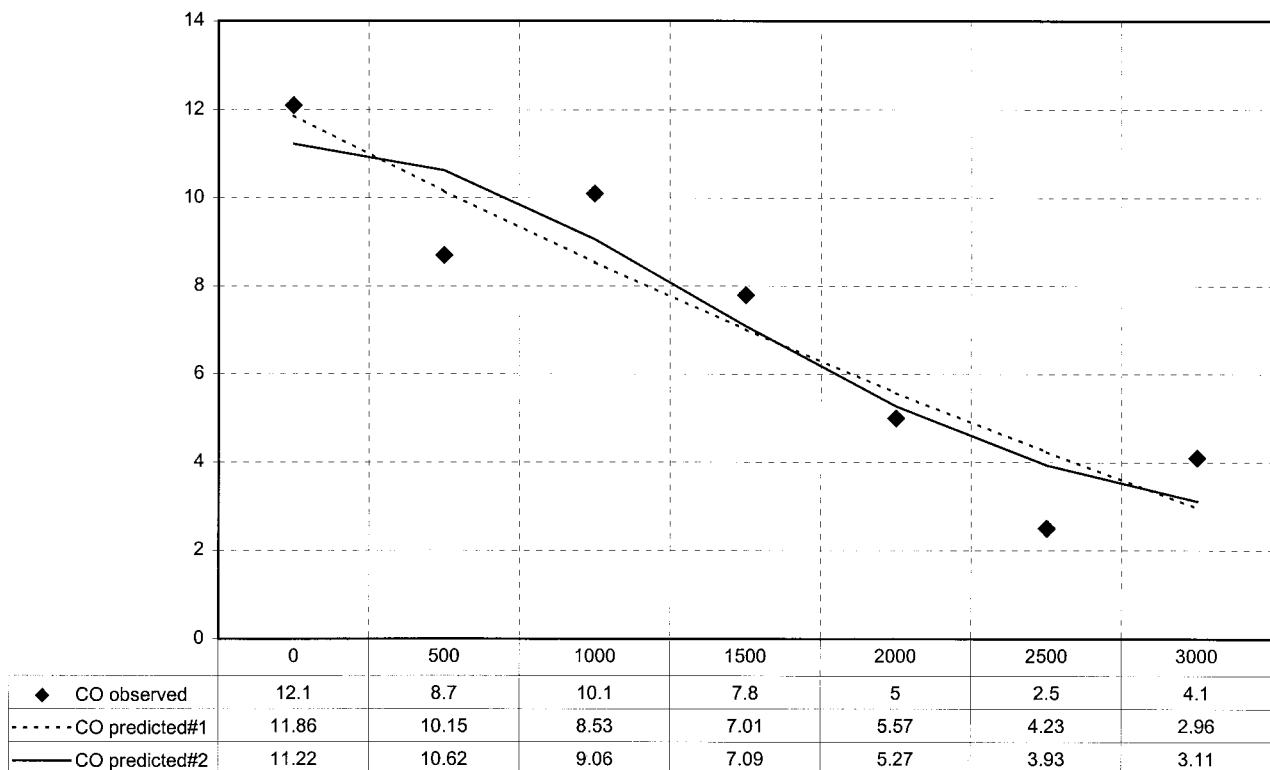
Figure 7 C—O by hours of xenon-arc exposure: curves and predictions of models 1 and 2.

CH2,C-C=O by Hours of Exposure

	0	500	1000	1500	2000	2500	3000
◆ CH2CCO observed	49.4	41.5	36.7	31.9	18.2	12.7	13.4
---- CH2CCO predicted#1	50.04	42.24	34.97	28.2	21.9	16.03	10.57
—— CH2CCO predicted#2	47.39	44.52	37.14	28.13	20.21	14.74	11.66
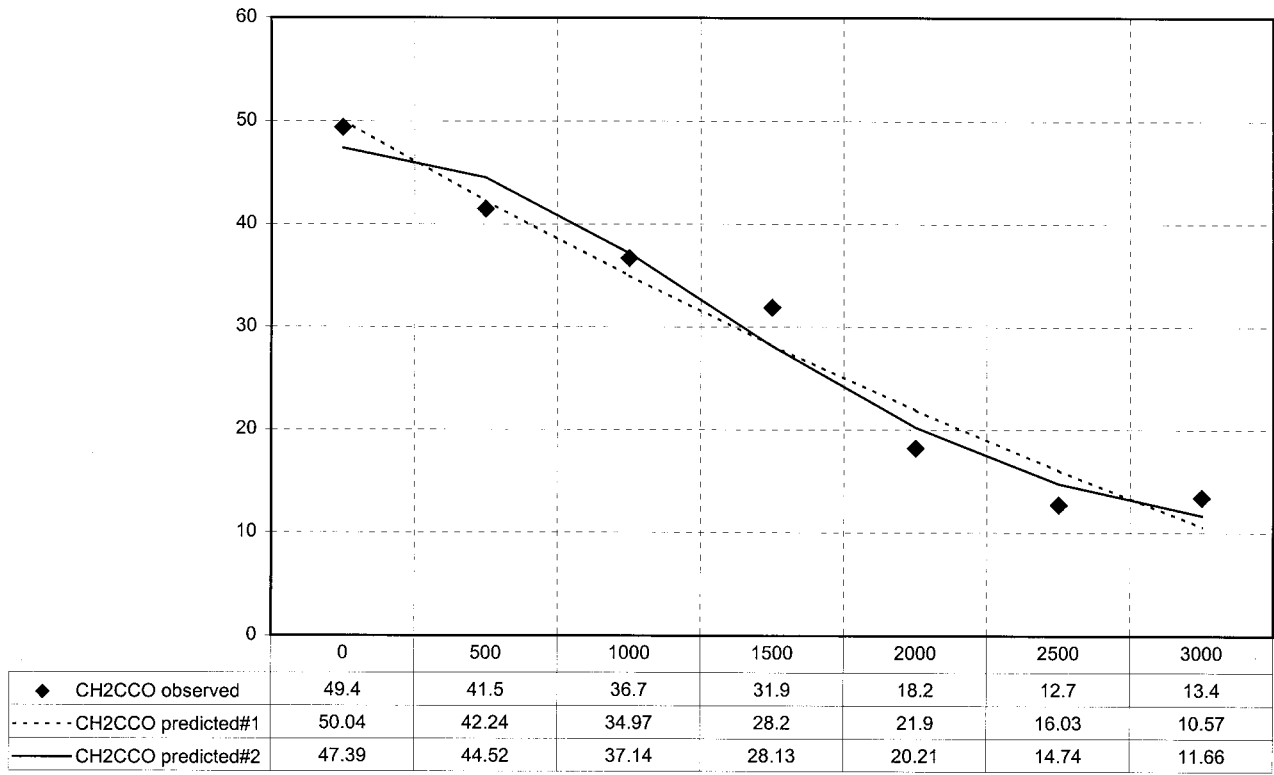
Figure 8 CH_2 + C—C=O by hours of xenon-arc exposure: curves and predictions of models 1 and 2.

Oxygen by Months of Exposure

	0	6	12	18	24	30	36	42	48
◆ O observed	23.4	21.3	33.9	42.1	56.6	57.7	58.5	59.4	61
---- O predicted#1	18.14	28.5	36.97	43.89	49.56	54.19	57.98	61.07	63.61
—— O predicted#2	20.46	24.34	33.87	44.52	52.72	57.46	59.6	60.36	60.58
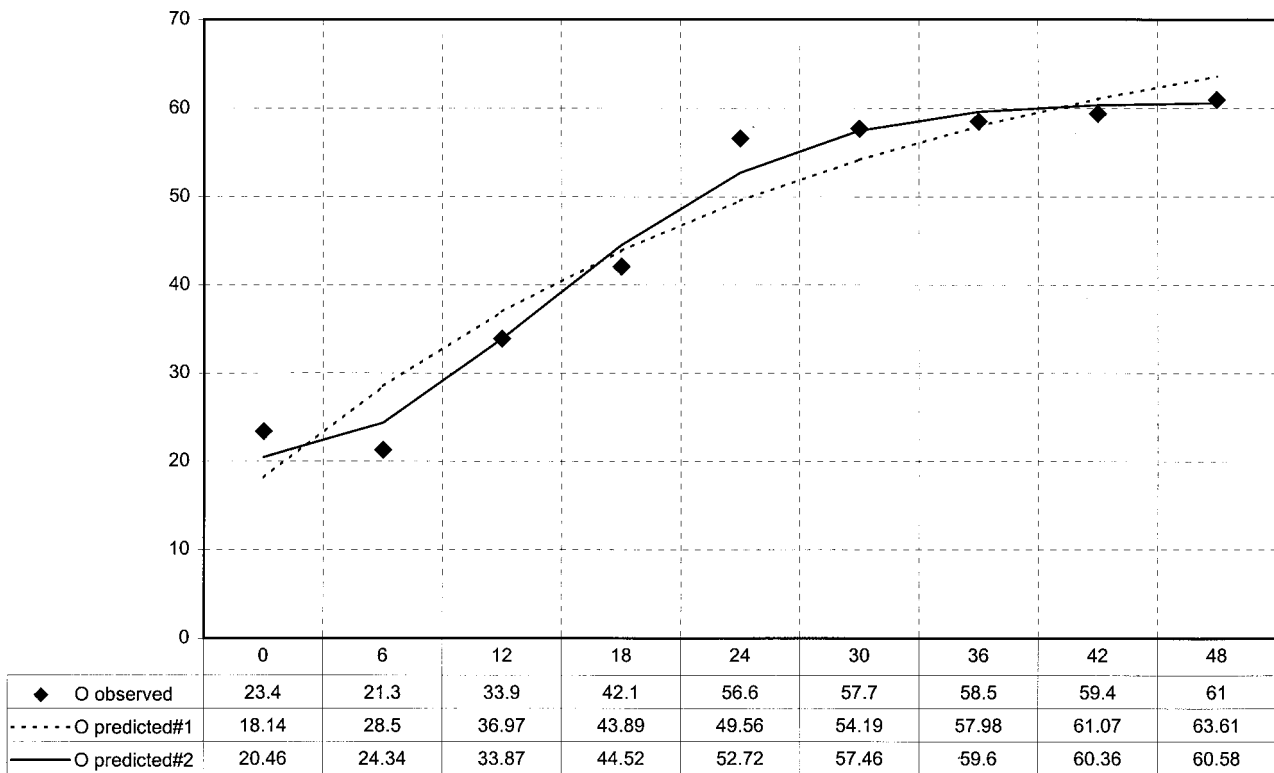
Figure 9   Oxygen by months of EMMAQUA exposure: curves and predictions of models 1 and 2.

Total Carbon by Months of Exposure

	0	6	12	18	24	30	36	42	48
◆ C observed	71.6	65.3	52.5	39.3	16.9	18.8	15.8	14.8	13.2
----- C predicted#1	76.56	59.79	46.61	36.26	28.12	21.73	16.71	12.76	9.66
—— C predicted#2	72.12	66.03	51.31	35.38	23.7	17.37	14.74	13.89	13.67

Figure 10 Total carbon by months of EMMAQUA exposure: curves and predictions of models 1 and 2.

Ratio of Oxygen to Carbon by Months of Exposure

	0	6	12	18	24	30	36	42	48
◆ O/C observed	0.327	0.326	0.646	1.071	3.349	3.069	3.703	4.014	4.621
----- O/C predicted#1	0.237	0.477	0.793	1.210	1.762	2.494	3.470	4.786	6.585
—— O/C predicted#2	0.284	0.369	0.660	1.258	2.224	3.308	4.043	4.346	4.432

Figure 11 O/C by months of EMMAQUA exposure: curves and predictions of models 1 and 2.

Nitrogen by Months of Exposure

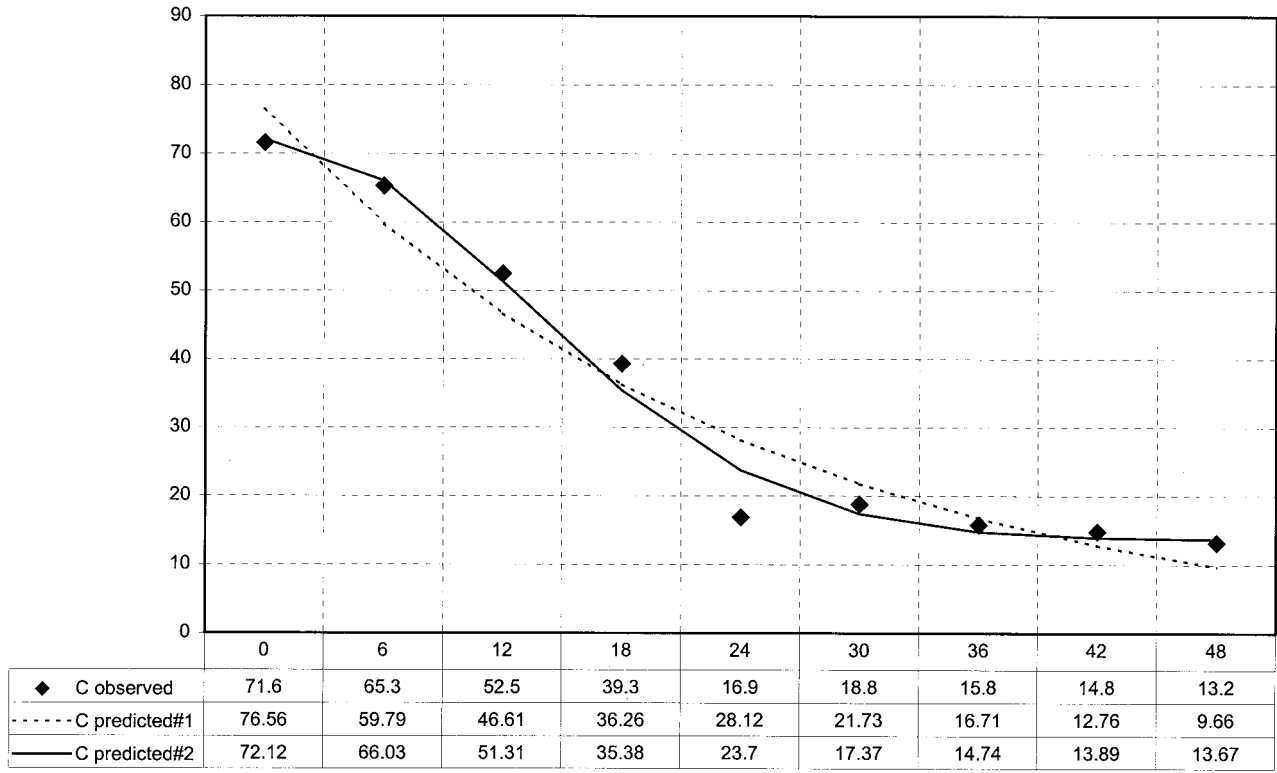|	0	6	12	18	24	30	36	42	48
◆ N observed	0	6.9	5.4	4.2	1.3	1	1.2	0.9	0.4
- - - N predicted#1	10.4	7.21	4.97	3.4	2.29	1.52	0.98	0.6	0.33
—— N predicted#2	7.72	7.05	5.38	3.51	2.06	1.2	0.81	0.66	0.62
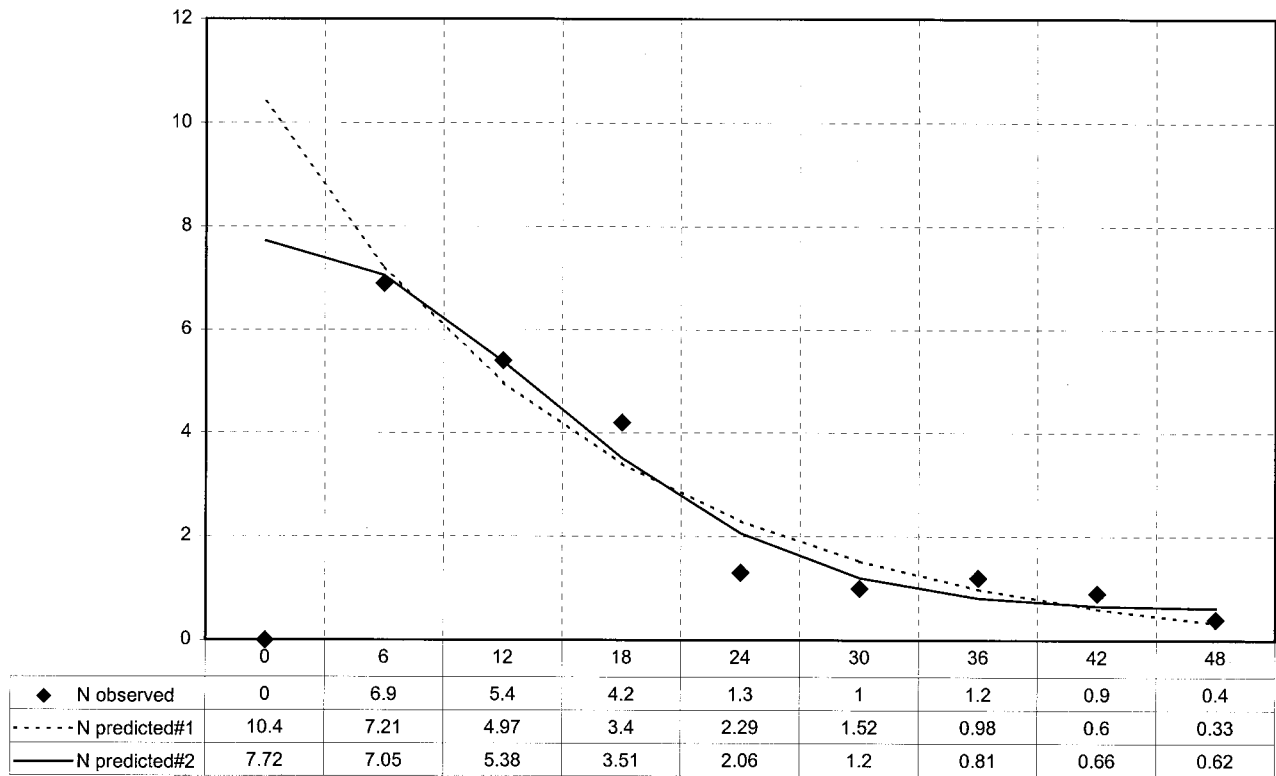
Figure 12   Nitrogen by months of EMMAQUA exposure: curves and predictions of models 1 and 2.
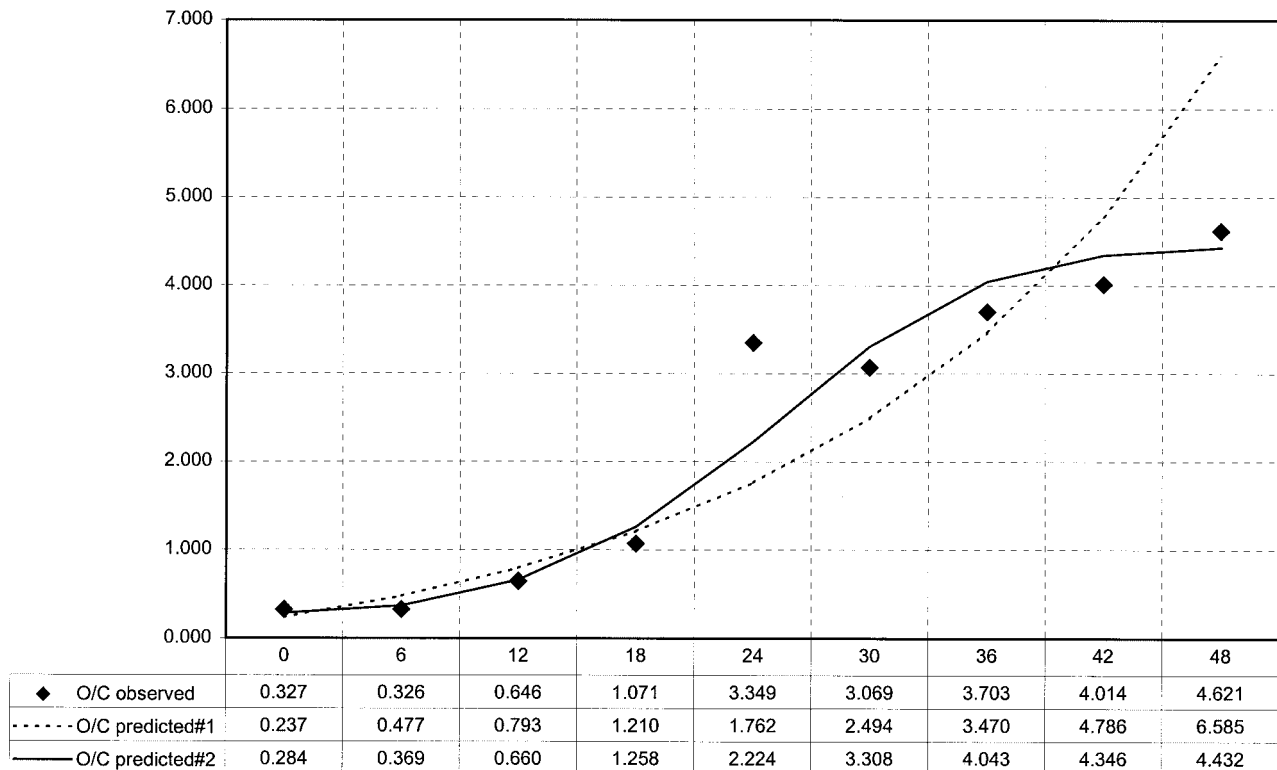
Ratio of Nitrogen to Carbon by Months of Exposure

	0	6	12	18	24	30	36	42	48
◆ N/C observed		0.106	0.103	0.107	0.077	0.053	0.076	0.061	0.030
- - - N/C predicted#1	0.136	0.121	0.107	0.094	0.081	0.070	0.059	0.047	0.034
—— N/C predicted#2	0.107	0.107	0.105	0.099	0.087	0.069	0.055	0.048	0.045
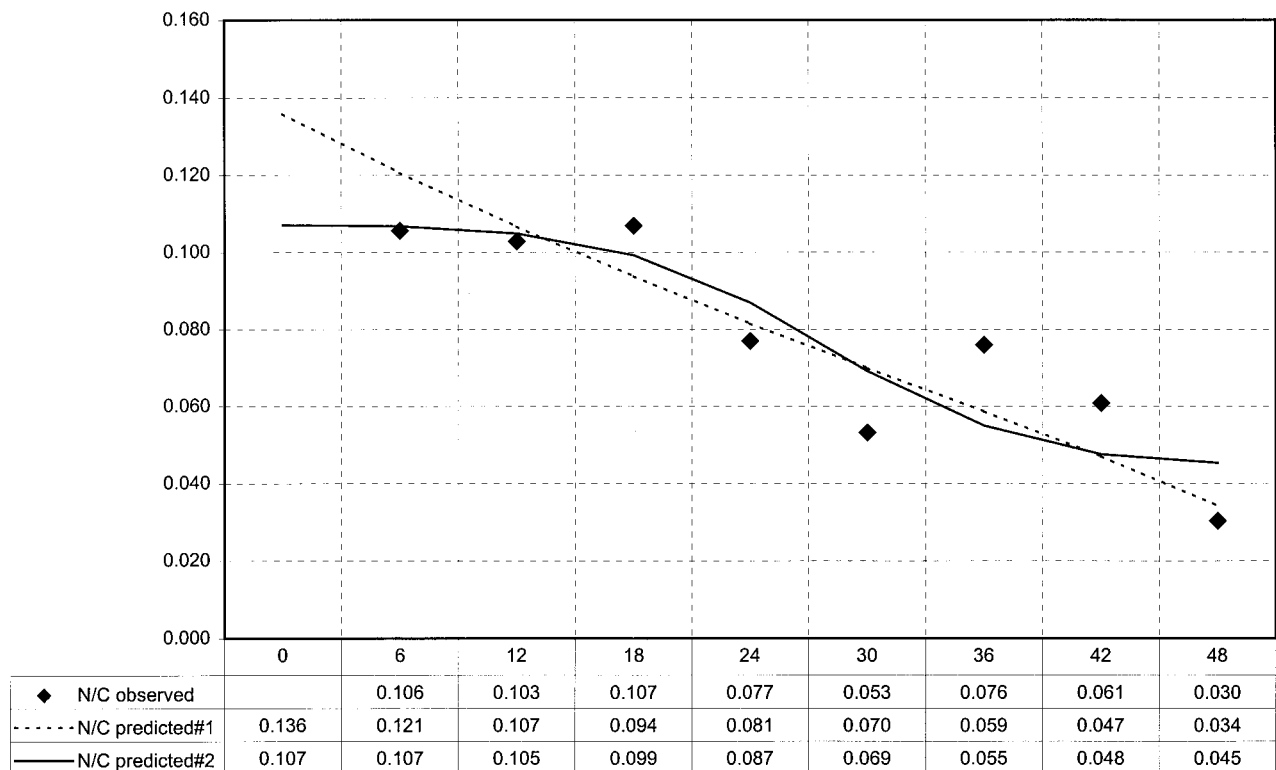
Figure 13   N/C by months of EMMAQUA exposure: curves and predictions of models 1 and 2.

O-C=O by Months of Exposure

	0	6	12	18	24	30	36	42	48
◆ OCO observed	10.1	13	10.3	7.9	3.2	2.8	3.1	2.6	2.3
···· OCO predicted#1	12.4	10.41	8.63	7.04	5.63	4.37	3.24	2.24	1.34
—— OCO predicted#2	12.18	11.4	9.39	6.97	4.86	3.43	2.64	2.28	2.15
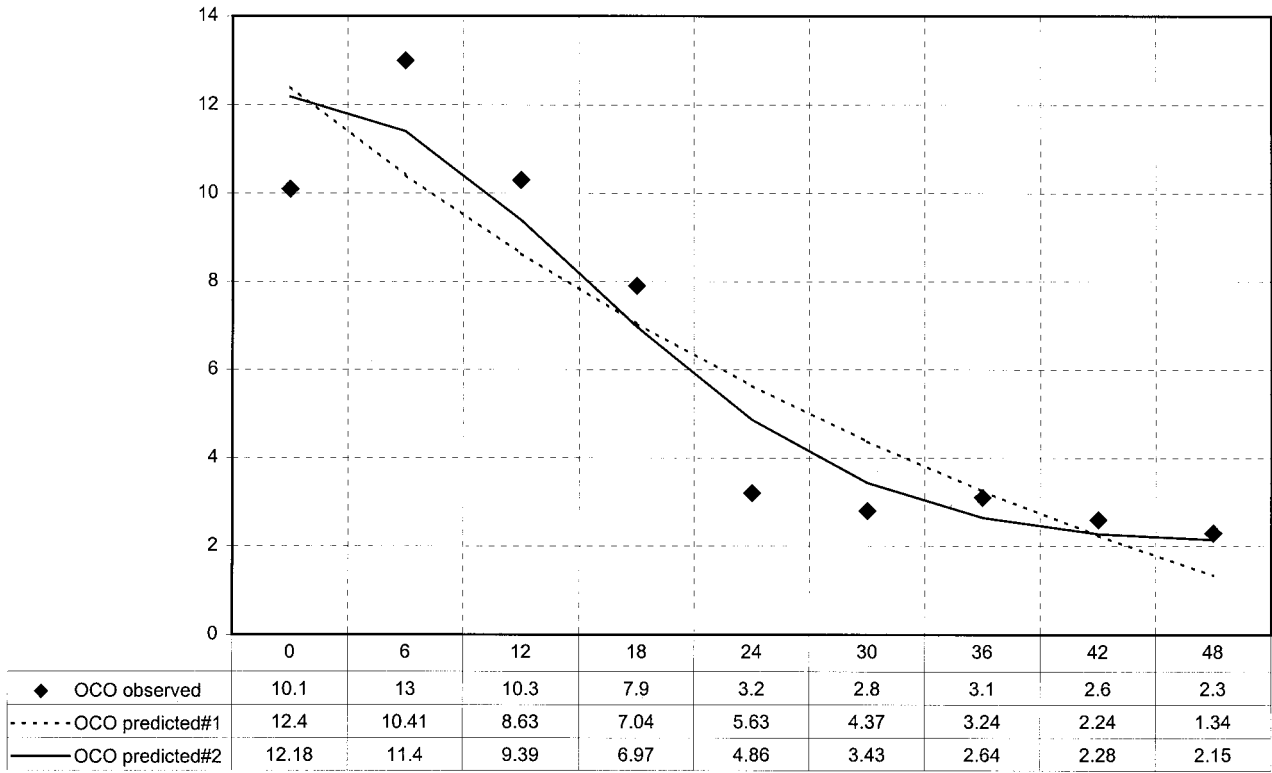
Figure 14   O—C=O by months of EMMAQUA exposure: curves and predictions of models 1 and 2.

C-O by Months of Exposure

	0	6	12	18	24	30	36	42	48
◆ CO observed	12.1	12.2	9.9	4.9	2.5	2.4	3.6	2.5	2.5
···· CO predicted#1	13.53	10.29	7.85	6.01	4.62	3.58	2.79	2.19	1.75
—— CO predicted#2	13.04	11.67	8.55	5.51	3.61	2.79	2.52	2.46	2.45
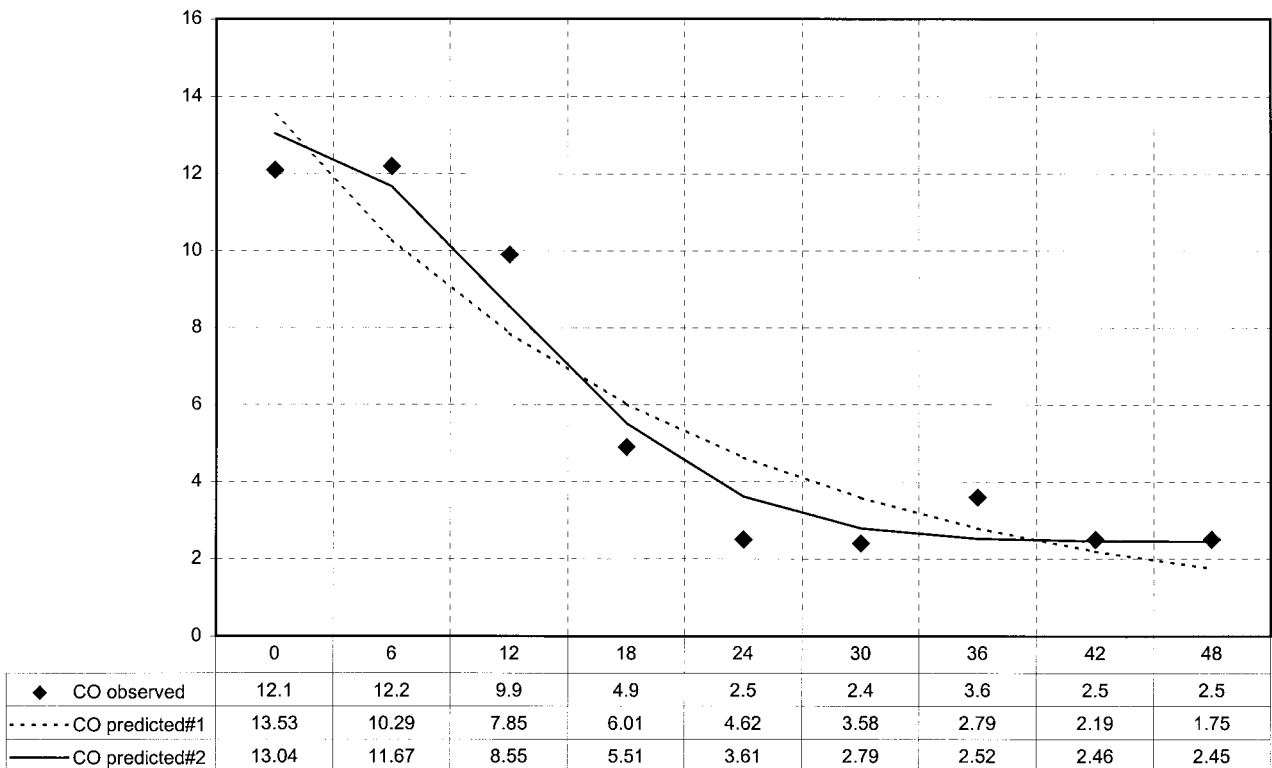
Figure 15   C—O by months of EMMAQUA exposure: curves and predictions of models 1 and 2.

CH2,C-C=O by Months of Exposure

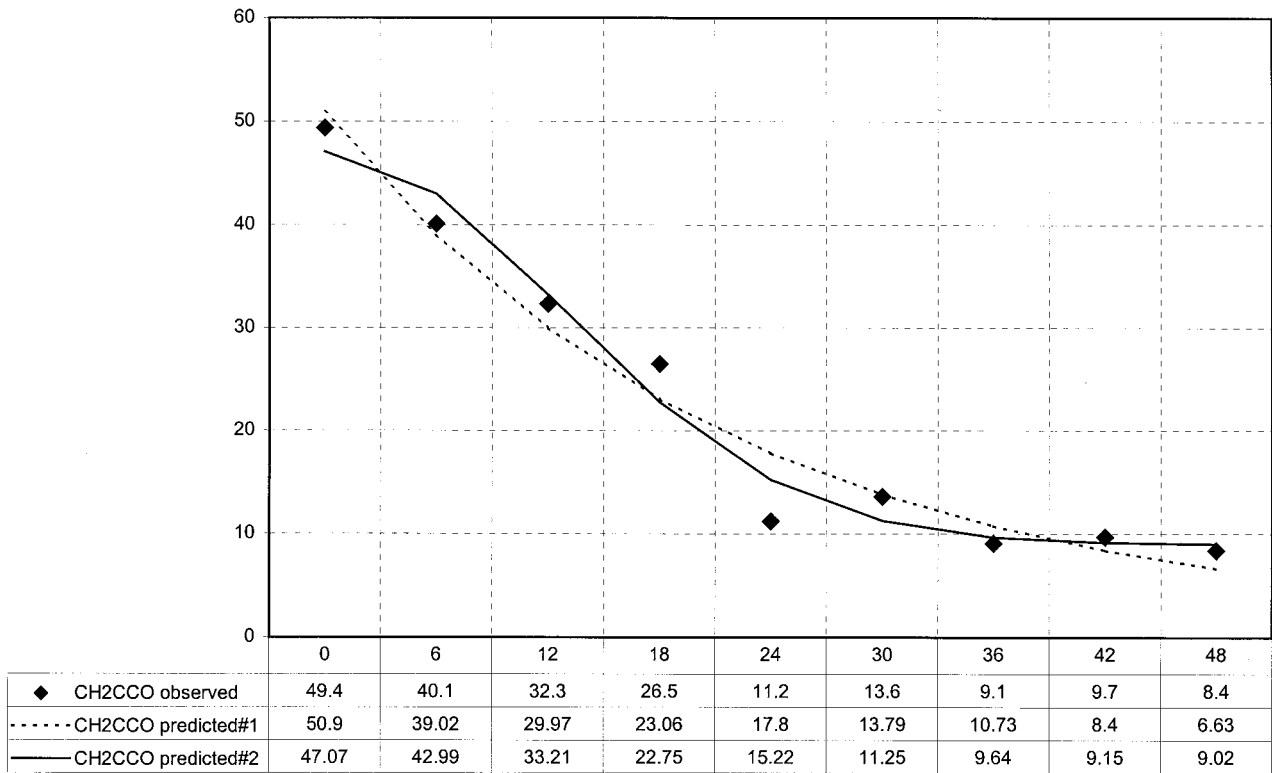|	0	6	12	18	24	30	36	42	48
◆ CH2CCO observed	49.4	40.1	32.3	26.5	11.2	13.6	9.1	9.7	8.4
----CH2CCO predicted#1	50.9	39.02	29.97	23.06	17.8	13.79	10.73	8.4	6.63
——CH2CCO predicted#2	47.07	42.99	33.21	22.75	15.22	11.25	9.64	9.15	9.02

Figure 16 Oxygen by months of EMMAQUA exposure: curves and predictions of models 1 and 2.
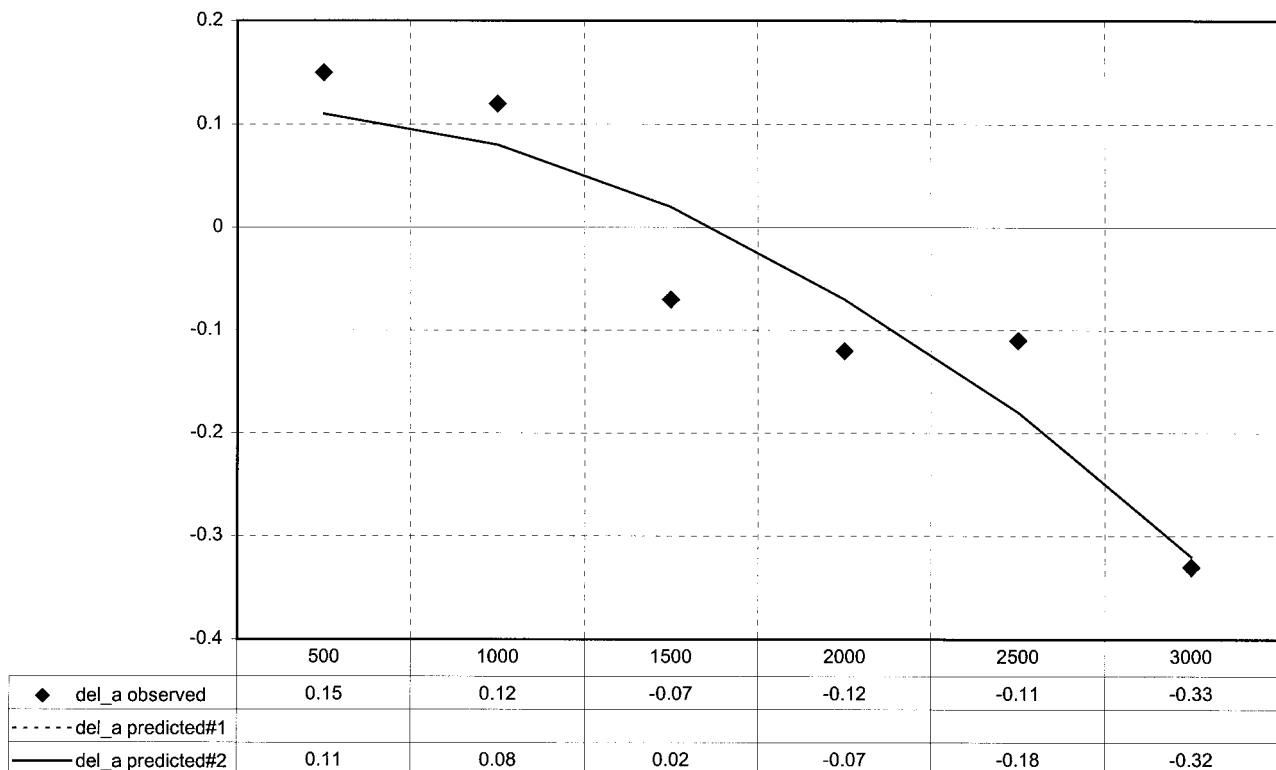
Change in "a" by Hours of Exposure

	500	1000	1500	2000	2500	3000
◆ del_a observed	0.15	0.12	-0.07	-0.12	-0.11	-0.33
----del_a predicted#1						
——del_a predicted#2	0.11	0.08	0.02	-0.07	-0.18	-0.32

Figure 17 Δa^* by hours of xenon-arc exposure: curves and predictions of models 1 and 2.

Change in "b" by Hours of Exposure

	500	1000	1500	2000	2500	3000
◆ del_b observed	0.87	1.34	1.64	1.96	2.13	2.41
------ del_b predicted#1	1	1.28	1.57	1.86	2.16	2.47
—— del_b predicted#2	1.18	1.29	1.48	1.75	2.11	2.56

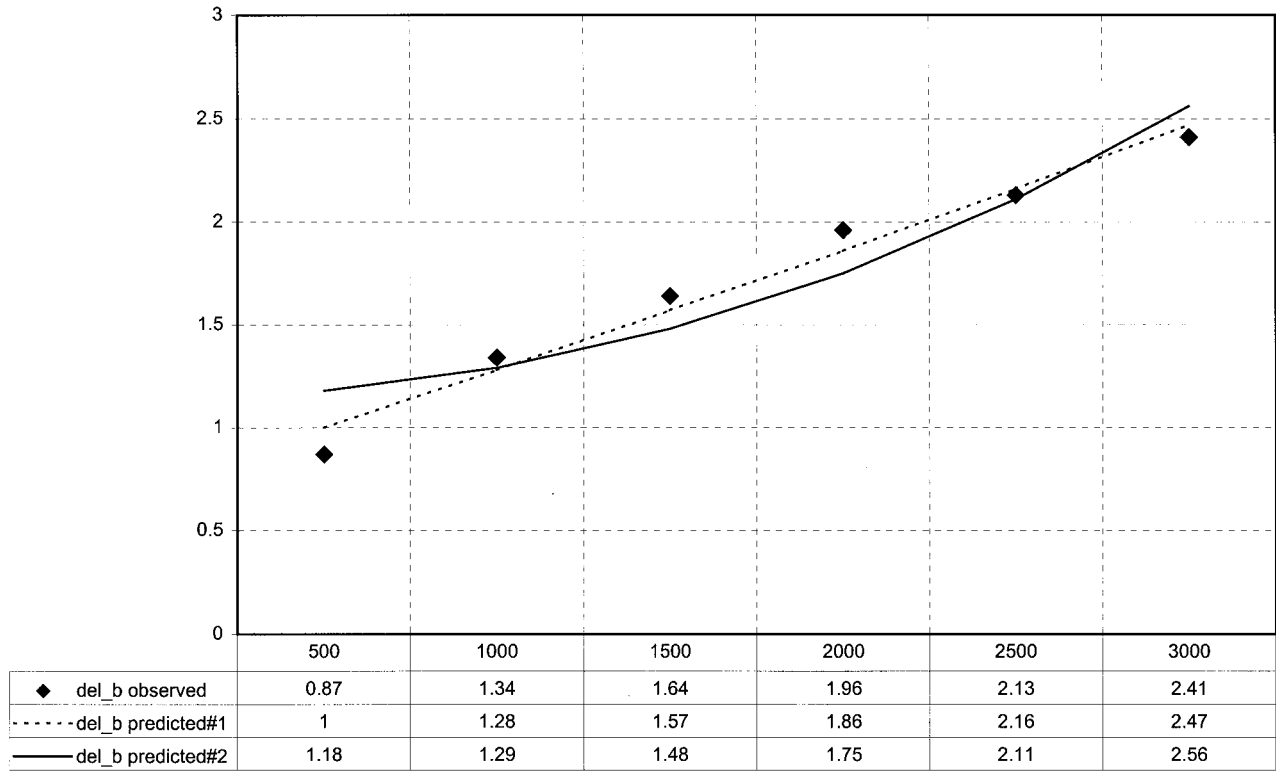**Figure 18** Δb^* by hours of xenon-arc exposure: curves and predictions of models 1 and 2.

Change in "L" by Hours of Exposure

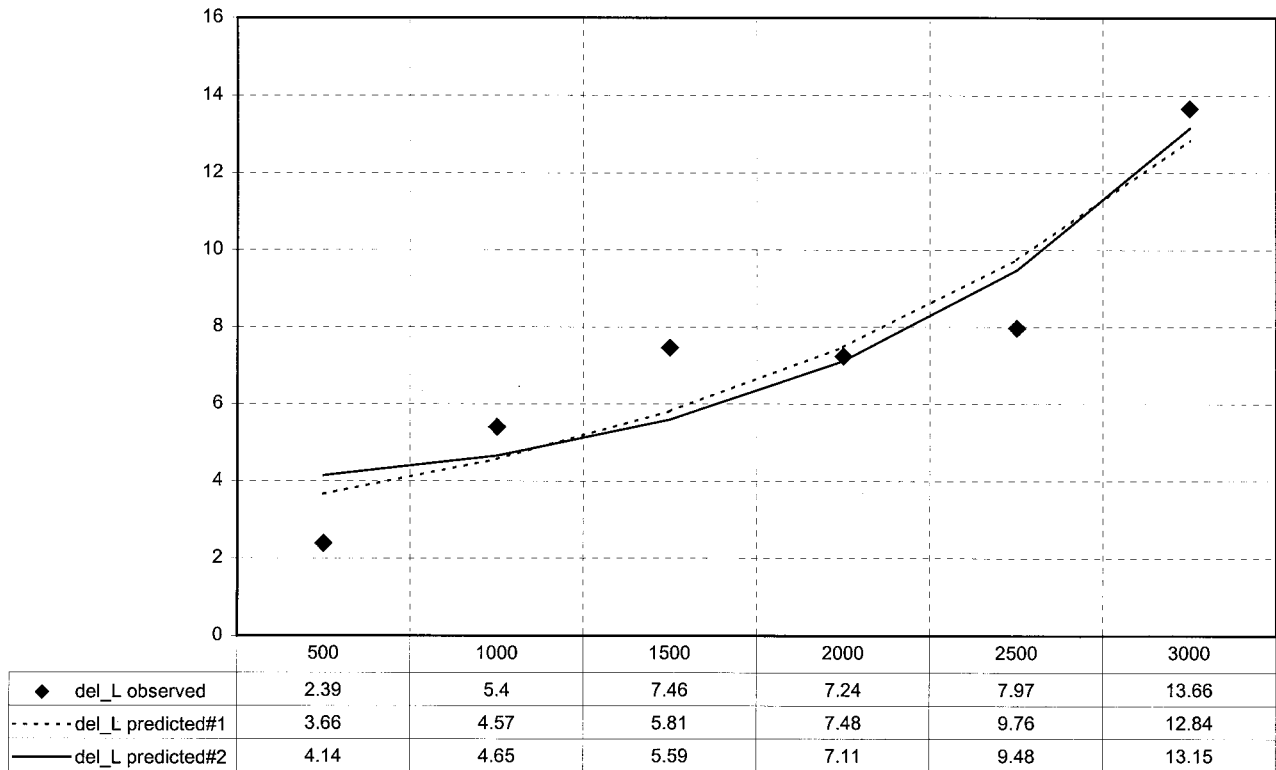|	500	1000	1500	2000	2500	3000
◆ del_L observed	2.39	5.4	7.46	7.24	7.97	13.66
------ del_L predicted#1	3.66	4.57	5.81	7.48	9.76	12.84
—— del_L predicted#2	4.14	4.65	5.59	7.11	9.48	13.15

Figure 19 ΔL^* by hours of xenon-arc exposure: curves and predictions of models 1 and 2.

Change in "E" by Hours of Exposure

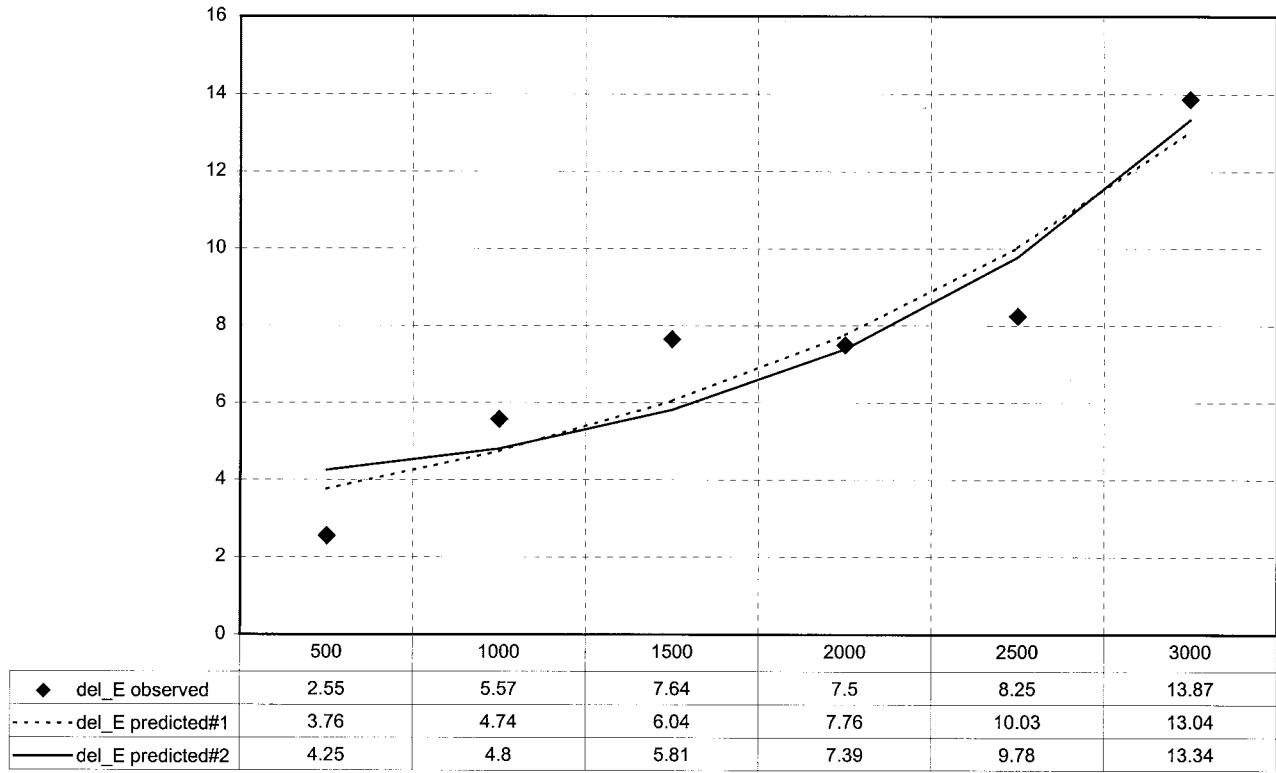| ◆	500	1000	1500	2000	2500	3000
del_E observed	2.55	5.57	7.64	7.5	8.25	13.87
del_E predicted#1	3.76	4.74	6.04	7.76	10.03	13.04
del_E predicted#2	4.25	4.8	5.81	7.39	9.78	13.34

Figure 20 ΔE by hours of xenon-arc exposure: curves and predictions of models 1 and 2.

Change in "a" by Months of Exposure

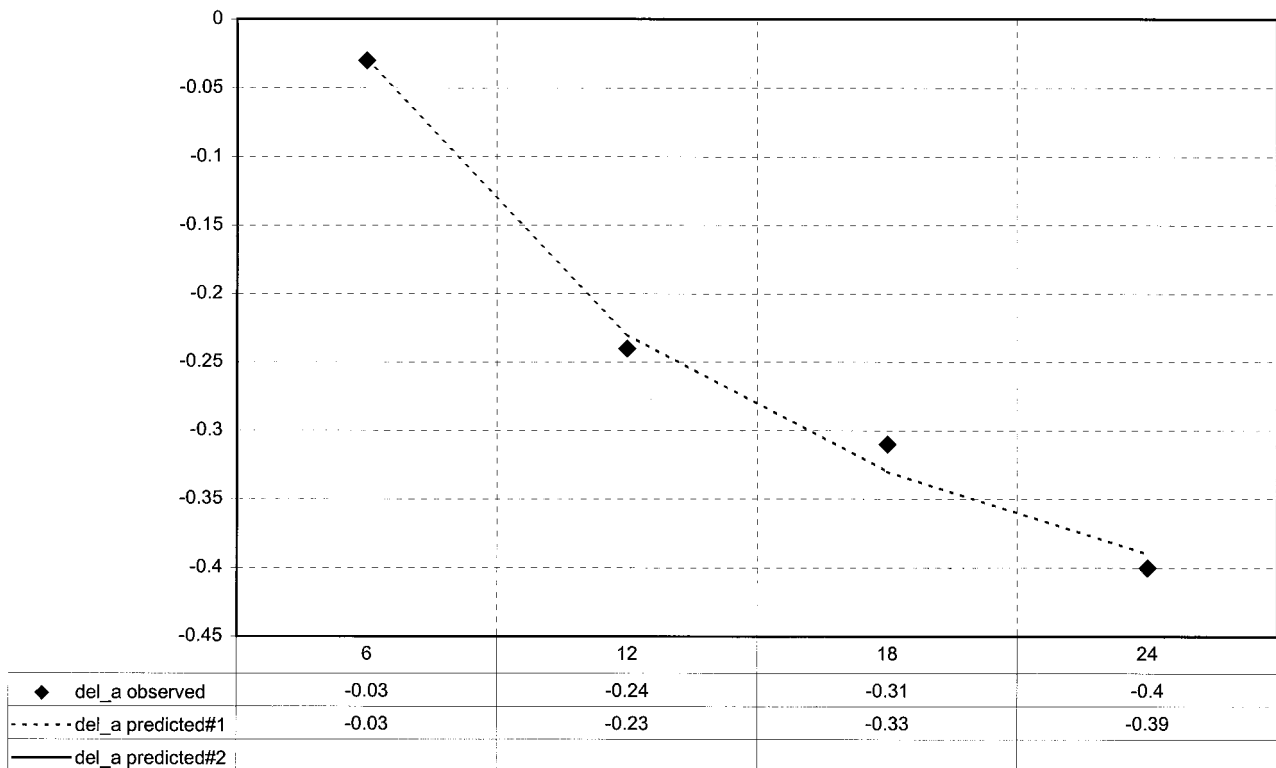| ◆	6	12	18	24
del_a observed	-0.03	-0.24	-0.31	-0.4
del_a predicted#1	-0.03	-0.23	-0.33	-0.39
del_a predicted#2				

Figure 21 Δa^* by months of EMMAQUA exposure: curves and predictions of models 1 and 2.

Change in "b" by Months of Exposure

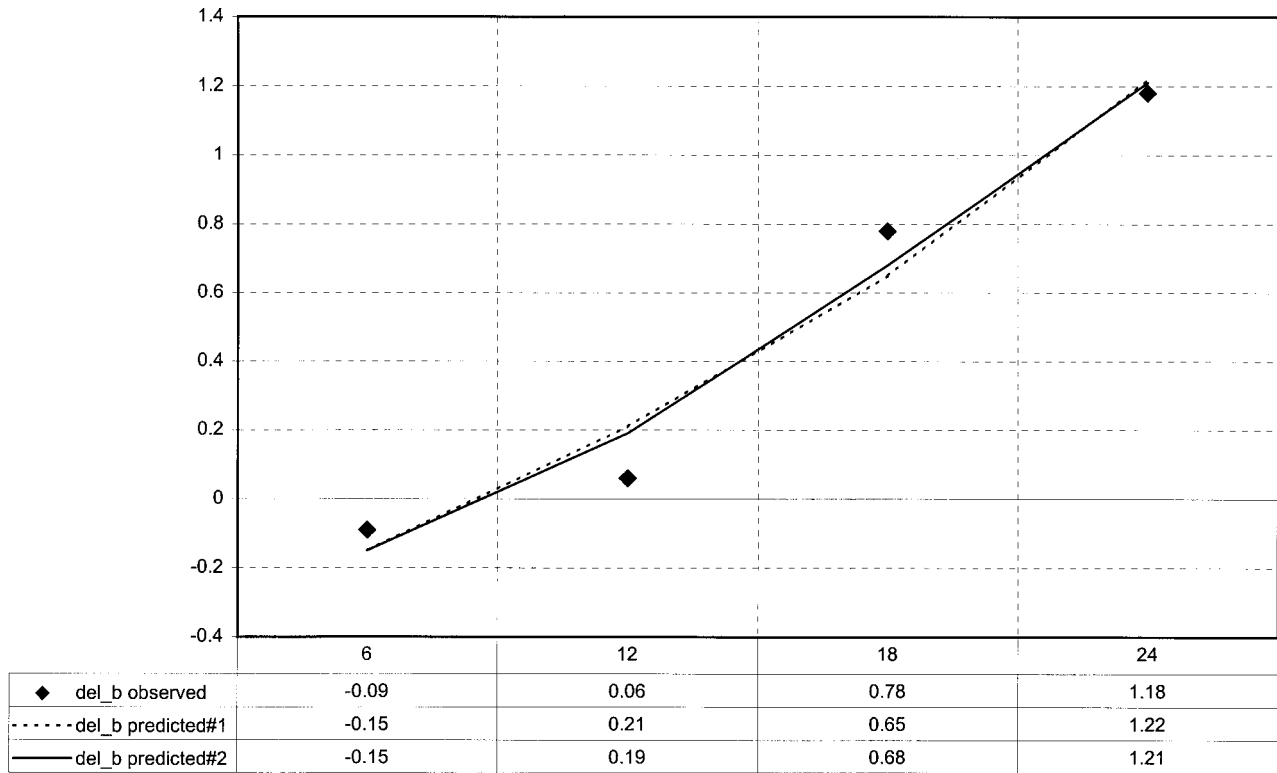|	6	12	18	24
◆ del_b observed	-0.09	0.06	0.78	1.18
del_b predicted#1	-0.15	0.21	0.65	1.22
del_b predicted#2	-0.15	0.19	0.68	1.21

Figure 22 $\Delta b*$ by months of EMMAQUA exposure: curves and predictions of models 1 and 2.

Change in "L" by Months of Exposure

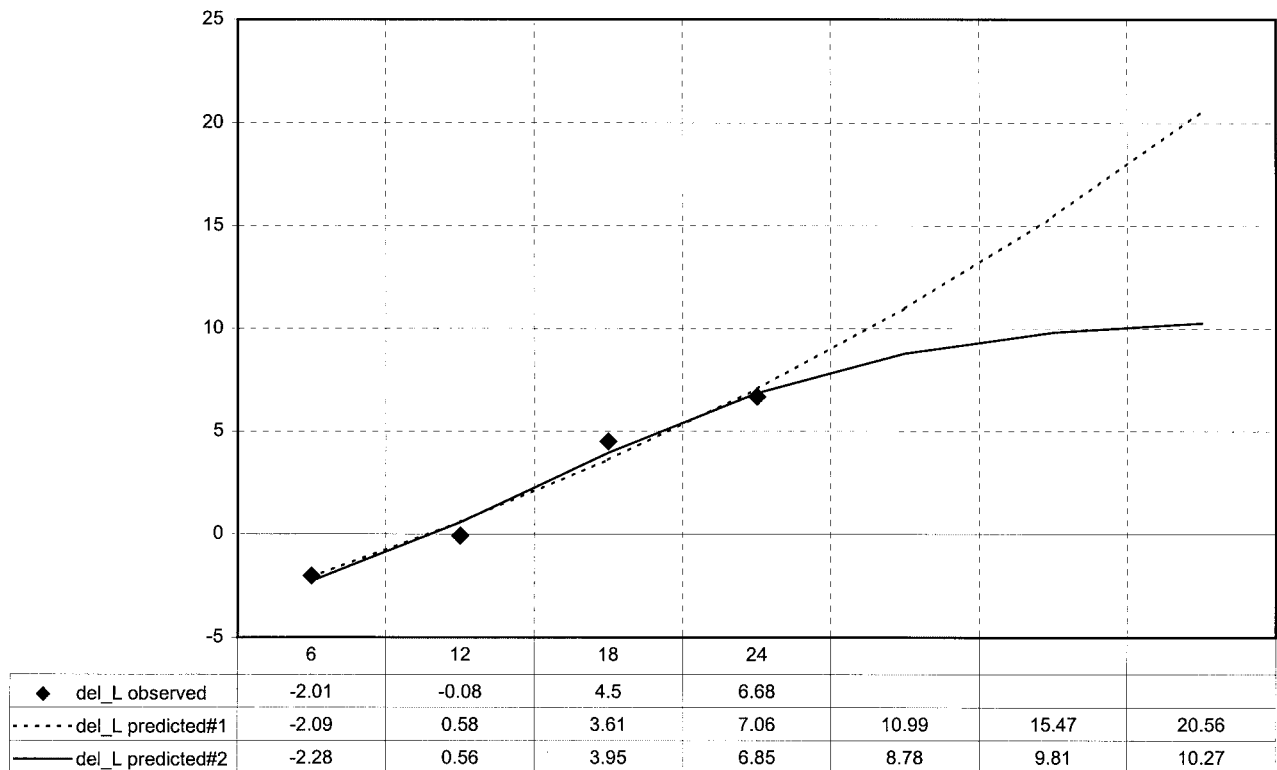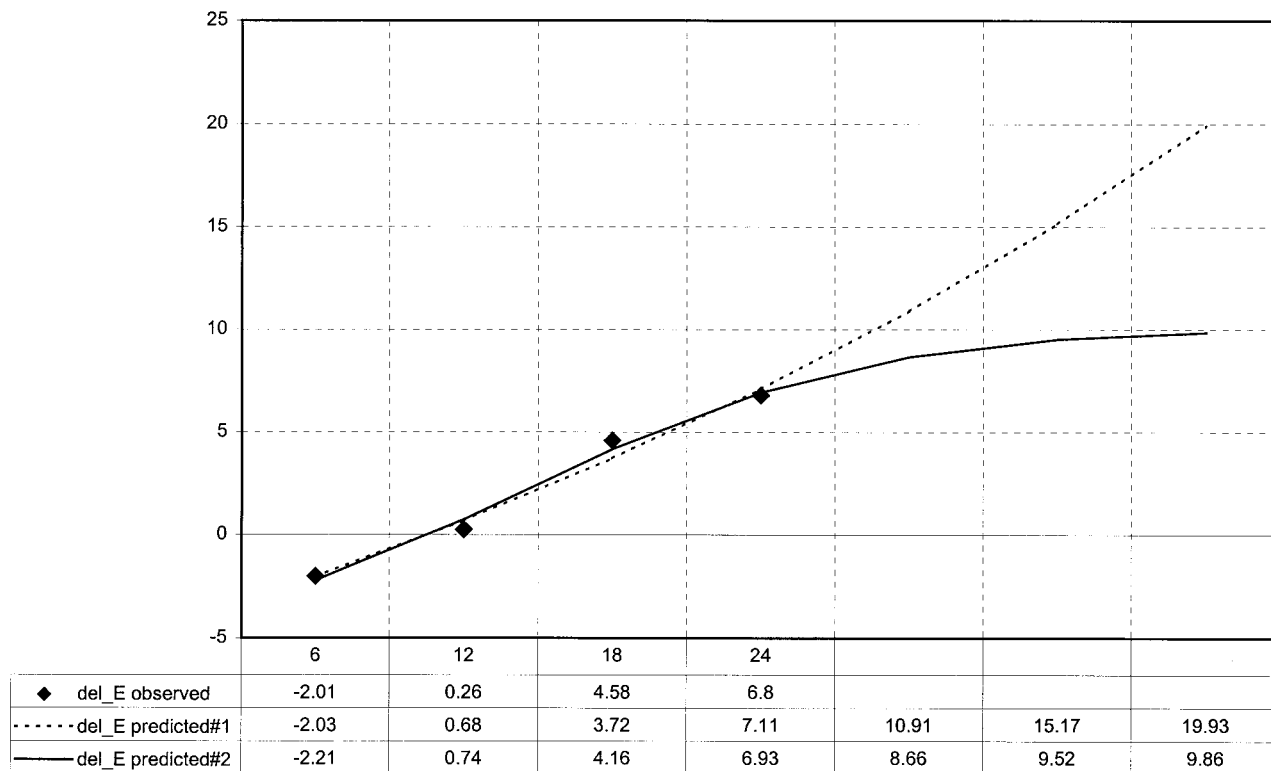|	6	12	18	24			
◆ del_L observed	-2.01	-0.08	4.5	6.68			
del_L predicted#1	-2.09	0.58	3.61	7.06	10.99	15.47	20.56
del_L predicted#2	-2.28	0.56	3.95	6.85	8.78	9.81	10.27

Figure 23 $\Delta L*$ by months of EMMAQUA exposure: curves and predictions of models 1 and 2.

Change in "E" by Months of Exposure

	6	12	18	24			
◆ del_E observed	-2.01	0.26	4.58	6.8			
· · · · del_E predicted#1	-2.03	0.68	3.72	7.11	10.91	15.17	19.93
—— del_E predicted#2	-2.21	0.74	4.16	6.93	8.66	9.52	9.86

Figure 24 ΔE by months of EMMAQUA exposure: curves and predictions of models 1 and 2.

RECOMMENDATIONS FOR FURTHER WORK

For statistical model development, specifically of the Weibull type, it is essential to obtain at least 5 and preferably 10 data points with respect to both analytical data and weather-o-meter exposure. We recommend that 10 XPS and color measurements should be made on each exposed sample to refine the Weibull-type and Gauss-type models. In addition, EMMAQUA exposures were found to fit the models much better than the xenon-arc exposures. Therefore, we should also replicate EMMAQUA exposures; 5 should be adequate.

TABLE IV
Asymptotic R^2 Statistics for Nonlinear Regressions

	Table I		Table II	
	Model 1 (h)	Model 2 (h)	Model 1 (months)	Model 2 (months)
ESCA (XPS) analysis				
O—C=O	0.843	0.926	0.821	0.913
C—O	0.862	0.872	0.876	0.960
CH$_2$, C—C=O	0.960	0.969	0.962	0.973
Total carbon	0.947	0.968	0.943	0.985
Oxygen	0.942	0.964	0.922	0.980
Nitrogen	0.850	0.880	0.946	0.968
Oxygen/carbon	0.734	0.847	0.691	0.932
Nitrogen/carbon	0.616	0.557	0.775	0.766
	Model 1 (h)	Model 2 (h)	Model 1 (months)	Model 2 (months)
Color measurement				
Change in color coordinate a^*	n/a	0.881	0.989	—
Change in color coordinate b^*	0.975	0.878	0.961	0.970
Change in color coordinate L^*	0.870	0.859	0.971	0.983
Change in color index E	0.876	0.864	0.979	0.990

CONCLUSIONS

XPS and $L*a*b*$ color measurement data gave good Weibull-type and Gauss-type weathering predictive models. Our results will find utility in the long-term performance results of aircraft coatings; in the design of newer, longer lasting aircraft coatings; in the evaluation of newly designed coatings; in the qualification of new aircraft coatings; and in repainting schedule determinations.

References

1. Dulog, L.; Saupp, U. Farbe Lack 1993, 99, 591.
2. Nagai, M.; Ogawa, M.; Tanida, O.; Yuneta, K.; Tanabe, H. Corrosion Control Conference, Seventh APCCC; International Academic: Beijing, 1991; Vol. 2.
3. Usmani, A. M. Usmani Development Company Final Report; Contract F33615-97-5094; Air Force Research Laboratory: WPAFB, OH, 1999.
4. Wicks, Z. W.; Jones, F. N.; Pappas, S. P. Organic Coatings; Wiley: New York, 1994; Vol. 2.
5. Baur, D. R. Ind Eng Chem 1991, 30, 2482.
6. Johnson, T. Eur Coat J 1996, 3, 106, 108, 110, 112, 406.
7. Schmelzer, J. FATIPEC 1994, 22, 59.
8. Usmani, A. M. In Coatings Science and Technology; Patsis, A. V.; Parfitt, G. D., Eds.; Marcel Dekker: New York, 1985; Vol. 8.
9. Saunders, J. H.; Frisch, K. C. Polyurethanes: Chemistry and Technology; Wiley: New York, 1962/1964; Vols. 1 and 2.
10. Dombrow, B. A. Polyurethanes; Reinhold: New York, 1957.
11. Usmani, A. M.; Salyer, I. O. Polym Plast Technol Eng 1979, 12, 61.
12. Usmani, A. M.; Donley, M. S. Polym News 2000, 25, 359.
13. U.S. Pat. 5,100,942 (1992).
14. U.S. Pat. 5,089,551 (1992).
15. U.S. Pat. 5,059,640 (1991).
16. U.S. Pat. 5,043,373 (1991).
17. U.S. Pat. 4,885,324 (1989).
18. Barr, T. L. Modern ESCA; CRC: Boca Raton, FL, 1994.
19. Practical Surface Analysis: Auger and X-Ray Photoelectron Spectroscopy; Briggs, D.; Seah, M. P., Eds.; Wiley: New York, 1996.
20. Practical Surface Analysis: Ion and Neutral Spectroscopy; Briggs, D.; Seah, M. P., Eds.; Wiley: New York, 1996.
21. Polymer Surfaces and Interfaces; Mittal, K. L.; Lee, K.-W., Eds.; VSP: Utrecht, 1997.
22. Genshaw, M. A. Color Res Appl 1985, 10, 235.
23. Degroff, J. T. Screen Graphic, Nov 1994.
24. Kamal, M. R. Polym Eng 1970, 10, 119.
25. Daiger, W. H.; Madson, W. H. J Paint Technol 1967, 39, 399.
26. Kamal, M. R. Polym Eng Sci 1966, 6, 333.
27. Hamid, S. H.; Amin, M. B. J Appl Polym Sci 1995, 55, 1385.